



# Pseudo-climate modelling study on projected changes in extreme extratropical cyclones, storm waves and surges under CMIP5 multi-model ensemble: Baltic Sea perspective

Martin Mäll<sup>1</sup> · Ryota Nakamura<sup>2</sup> · Ülo Suursaar<sup>3</sup> · Tomoya Shibayama<sup>1</sup>

Received: 30 March 2019 / Accepted: 25 March 2020 / Published online: 4 April 2020  
© Springer Nature B.V. 2020

## Abstract

In order to estimate the possible parameters of future extreme extratropical cyclones (ETCs), a pseudo-climate modelling study of three historical storms originating from the Atlantic Ocean and one from the Black Sea area was performed using multi-model approach considering IPCC emission scenarios RCP4.5 and RCP8.5 for the twenty-first century. Applying Weather Research and Forecasting atmosphere model (WRF), Finite Volume Community Ocean model (FVCOM-SWAVE) and the Simulating WAVes Nearshore (SWAN) model, the changes in initial conditions in atmospheric air temperature, sea surface temperature and relative humidity were considered on the basis of 14 CMIP5 general circulation models ensemble. According to the future scenario results, no notable changes are expected in minimum atmospheric pressure within the ETCs of the future; however, the low pressure area was slightly larger and the strong wind zone was extending further south with greater peak wind speeds in the future (year 2081–2100) simulations. This, in turn, yielded a small surge height increase at Pärnu under RCP4.5 scenario; however, under RCP8.5 scenario the surge increase was up to 22–59 cm. Westerly approaching ETCs will bring more precipitation to the Baltic Sea area in the (warmer) future. In case of a southerly cyclone, the results were more mixed. An insignificant increase in wave heights during extreme storm conditions occurred. Although RCP8.5 future scenario is usually considered as unrealistic, the results of this study still suggest that the extreme ETCs may become more dangerous in the future, although probably not as certainly as tropical cyclones.

**Keywords** FVCOM-SWAVE · ETC · Cyclone tracks · Sea level · Storm surge · Precipitation · Climate change

---

✉ Martin Mäll  
mallmartin4@gmail.com

<sup>1</sup> Department of Civil and Environmental Engineering, Waseda University, 3-4-1 Okubo, Shinjuku-ku, Tokyo 169-8555, Japan

<sup>2</sup> Civil Engineering Program, Faculty of Engineering, Niigata University, 8050, Ninocho, Nishi-ku, Niigata-shi, Niigata 950-2181, Japan

<sup>3</sup> Estonian Marine Institute, University of Tartu, Mäealuse 14, 12618 Tallinn, Estonia

## 1 Introduction

In Europe, much of the high-impact weather events are associated with extratropical cyclones (ETCs; e.g. Feser et al. 2015). In addition to impacts as windstorms, ETCs have caused heavy precipitation and storm surges in many coastal areas, including the Baltic Sea (Averkiev and Klevanny 2010; Wolski et al. 2014). Coastal zones are highly vulnerable to changes in Earth climate system, firstly, due to anticipated mean sea level rise, and secondly, regarding changes in storm activity. Concurrent impacts are inundation of low-lying urban areas, coastal erosion, damage to infrastructure or even loss of life (Emanuel 2005). The activity of ETCs is a dominant feature anywhere in the mid-latitudes during the period from autumn to spring (Mizuta 2012); any change in this activity due to global warming would have a marked influence on socio-economic and ecological systems, as well as the daily lives of many people (Hoegh-Guldberg and Bruno 2010). However, the discussion on changes in storminess is still full of controversies. There is no overall agreement on whether the frequency and intensity of storms has increased or will increase in the future. According to many researchers, climate variability and uncertainty has grown over the last 50 years (Stainforth et al. 2005) and extreme weather events are becoming more violent (Emanuel 2005; Matulla et al. 2008). However, other studies have indicated that compared to the sample size, the natural variability of storms is large (Trenberth 2005) and the data series are frequently just plagued by inhomogeneities (Van Gelder et al. 2008). In this study, the authors attempt to cast new insight to the problem of future ETCs.

Current projections on future changes in winds and ETCs are somewhat mixed (Pinto et al. 2011; Christensen et al. 2015), and the question is still open, whether the ETCs become stronger under the rising temperatures above the Northern Atlantic or not. For instance, most models project a steady decrease in the number of ETCs for the US East Coast and North-western Atlantic region by the late twenty-first century, while showing increase in more intense cyclones and heavy precipitation events (Colle et al. 2015). However, there is also a large inter-decadal variability and potential biases may exist in the models because of difficulty in capturing the Atlantic storm track sensitivity to the Gulf Stream sea surface temperature gradient, latent heating within the storms and dynamical interactions at jet level (Woollings et al. 2010; Martin 2006). Whereas, in contrast, it is highly possible that at least tropical cyclones will get stronger as a result of further climate warming (Knutson and Tuleya 2004).

In the Baltic Sea region, which is the main study area for the current study, the increase in storminess has been observed over the last 50 years (e.g. Gregow et al. 2012), however not over the longer, 100–150 years period (e.g. Weisse et al. 2009). Those observed changes are largely related to the northward shift and eastward extension of the storm tracks (Ulbrich et al. 2009; Zappa et al. 2013b), which also means that time-varying and different, even contrasting, tendencies above Southern and Northern Europe are possible. Cyclones affecting the Baltic Sea may propagate along several distinct tracks. A large and probably the most influential part of such atmospheric low pressure systems is formed (mainly during the colder half of the year) near the polar front in the Northern Atlantic Ocean, between Iceland, Greenland and Newfoundland Peninsulas. They track eastwards across the British Isles and Central Scandinavian Peninsula along westerly or south-westerly routes (Suur-kaar et al. 2018). A second distinct group of cyclones are the ones that cross over the Bay of Biscay, France and Germany. And the third is of south-southeastern origin that brings, especially in summer, much of the precipitation and lightning (Mändla et al. 2015). Occasionally, cyclones may also approach from north, however rarely from the east.

The impacts of storms are always strongly dependent on storm track in relation to coast-line configuration, bathymetry and other factors (Tasnim et al. 2015). For instance, a truly remarkable storm making its landfall on straight and sparsely populated coast may have a smaller impact than the one which happens to hit a heavily indented, low-lying and densely populated coastal areas. Thus, the physical intensity of a storm does not necessarily coincide with the severity of the event in terms of environmental or societal impact. Extreme sea levels can sometimes occur due to a favourable combination of factors, though within their normal range of variability. If the individual factors are statistically independent, the probability of the “perfect storm” or the most devastating storm surge can be so low, that it has not occurred yet within the measured history, although in principle it can happen at any time. For instance, in spite of the incredible damage hurricane Sandy caused in late October 2012, recent modelling studies demonstrated that Sandy’s storm surge was not the worst-case scenario for the New York area (Forbes et al. 2014). The same was in principle noticed for the cyclone Gudrun in the Baltic Sea in 2005 (Suursaar et al. 2006). Moreover, as a result of climate change and global sea level rise, the probability of one or more constituents for a perfect storm may be gradually changing for worse.

In recent decades, the changes in future storminess have been tried to study using various modelling approaches. For instance, there have been several, extensive climate modelling projects in Europe (e.g. EURO-CORDEX; Jacob et al. 2012; Vourdoukas et al. 2016), many of them enabling ensemble approaches. Lesser used in Europe is the approach which deals with individual events nested into hypothetical future. Historically, such an approach has been called a surrogate climate change modelling (Schär et al. 1996), and later, pseudo-climate change simulation (e.g. Patricola and Wehner 2018). It basically originates from a dynamical downscaling method which uses the idea of nesting a past notable event into hypothetical future with altered boundary conditions: perturbations from the circulation models future minus the historical are included in the reanalysis-derived initial and boundary conditions used in the control simulation (e.g. Kimura and Kitoh 2007; Kawase et al. 2009). Although the method is considered dynamically consistent (Patricola and Wehner 2018), it has some limitations and shortcomings, especially in relation to physics of cyclogenesis. For instance, it only adds thermodynamic changes to the WRF runs, but neither includes any variability to the occurrence of storms nor the possible influence of upstream teleconnections.

Using the Advanced Research Weather Research and Forecast model (ARW-WRF) and the Finite Volume Community Ocean model (FVCOM), Tasnim et al. (2015) simulated the historical cyclone Nargis (2008) and its storm surge under the future climate conditions (i.e. in 2100). They found that the cyclone would be stronger in the future and the storm surge in the Bay of Bengal much higher. Using a similar approach, however more advanced methodology, Nakamura et al. (2016) studied the storm and surge parameters of 2013 super-typhoon Haiyan. Although the degree of uncertainties for such calculations was fairly large (e.g. Nakamura et al. 2016), they mostly seemed to confirm that tropical cyclones could indeed get stronger under warming future climates.

Considering the aforementioned result on tropical cyclones and using the same modelling approach, it would be interesting to compare, what kind of alterations occur in ETCs under the rising temperatures in the Northern Europe. Mäll et al. (2017) presented an attempt to analyse the parameters and impacts of “future Gudrun”. ETC Gudrun (on 8–9 January 2005) being the most influential storm in Estonia’s recorded history, was a remarkable event elsewhere in Northern Europe as well. The accompanying record-high storm surge at Pärnu was analysed by Suursaar et al. (2006), and the coastal destruction was assessed by Tõnisson et al. (2008). Mäll et al. (2017) reconstructed the storm and modelled

the resultant storm surge at Pärnu by means of ARW-WRF and FVCOM modelling system. Then, they simulated “future Gudruns” for years 2050 and 2100, in accordance with the IPCC’s (Intergovernmental Panel on Climate Change) Fifth Assessment Report (AR5) proposed RCP4.5 and RCP8.5 climate change scenarios. The study showed that such a type of extratropical (polar front originated) cyclones, perhaps, may not get stronger under warming future climate conditions. For confirmation or rejection of such a finding, the same storm was reanalysed here again, using slightly improved methodology and finer input datasets. Analysing the “future Gudrun”, Mäll et al. (2017) concluded that more storm events with different tracks and from different seasons (i.e. thermal and baric background situations) should be analysed for more valid generalizations. In addition to storm Gudrun recalculation, the authors considered three other, rather different, cyclonic storm events (Fig. 1). The same improved data sources were used for other three storm events as well, therefore enabling their comparative analysis.

The aim of the current paper is to analyse the possible changes in ETCs behaviour under improved methodology, while also considering four different (tracks, thermal conditions) historical ETCs as case studies. New future conditions were derived from Coupled Model Intercomparison Project Phase 5 (CMIP5) 14 multi-model ensemble, where the changed parameters included atmospheric air temperature (AAT), sea surface temperature (SST)

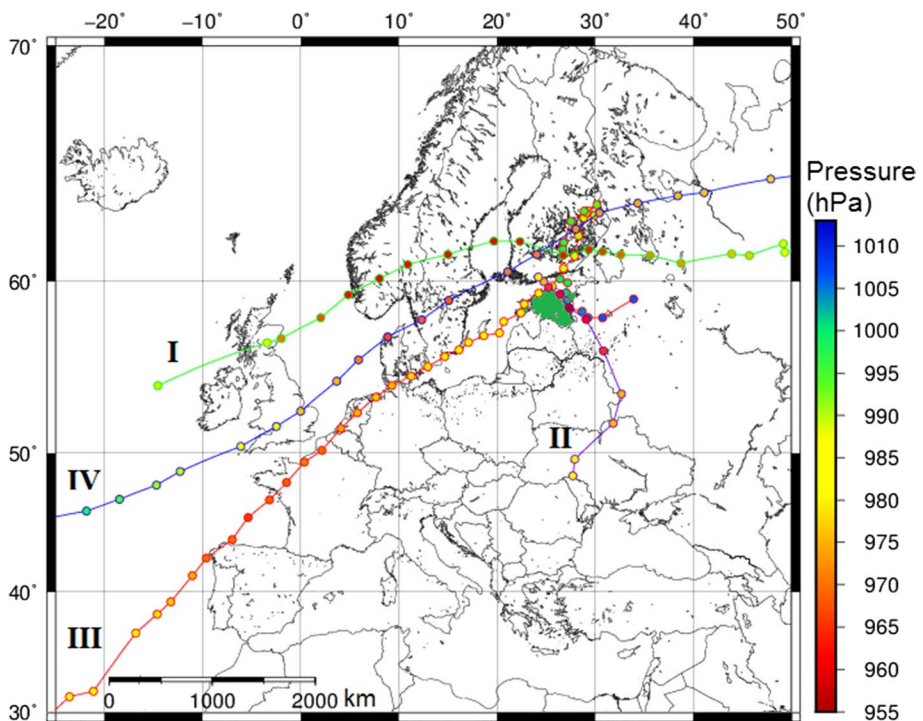


**Fig. 1** Tracks of four studied ETCs. I—January 2005 storm (“Gudrun”), II—November 2008 (snowstorm), III—February 2010 (“Xynthia”), IV—October 2013 (“St. Jude”). The colours in circles show MSLP values, and the location of Estonia is marked in green. The cyclone II actually originated more southward than shown; however, its track identification was complicated in earlier stages. Atlantic storm track data are from XWS Catalogue (Roberts et al. 2014), and 2008 storm track is compiled from pressure charts ([www.wetterzentrale.de](http://www.wetterzentrale.de))



and relative humidity (RH). Study scope was maintained within the Baltic Sea region, and more detailed analysis was performed for Estonia. The changes in future cyclone behavior under different tracks, forming conditions and impacts are discussed on a regional to local-scale.

## 2 Materials and methods

### 2.1 The modelling system

The modelling approach within this study framework was similar to that of Mäll et al. (2017) and more in-depth details about the approach can be found from there. However, in this study, some considerable improvements have been made to make use of the highest quality of data to mitigate data-related potential biases. The main tools of the current research were the ARW-WRF atmospheric model (ver. 3.9.1.1; Skamarock et al. 2008) for simulating the atmospheric conditions throughout the investigated storms life cycle, and the updated FVCOM ocean model (ver. 4.1), including the wave-current interaction (hereafter: FVCOM-SWAVE; Chen et al. 2003; Qi et al. 2009; Wu et al. 2010), for simulating sea level variations along the West coast of Estonia. Furthermore, the SWAN model version 41.20 (Booij et al. 1999; Björkqvist et al. 2018) was used to simulate the future changes in significant wave heights ( $H_s$ ) and its spatial distributions inside the Baltic Sea.

The modelling framework (Fig. 2) applied top-down approach. The initial step was to run the atmospheric model WRF in order to validate the accuracy of the model output. To control the modelling biases between four different storm cases, the authors

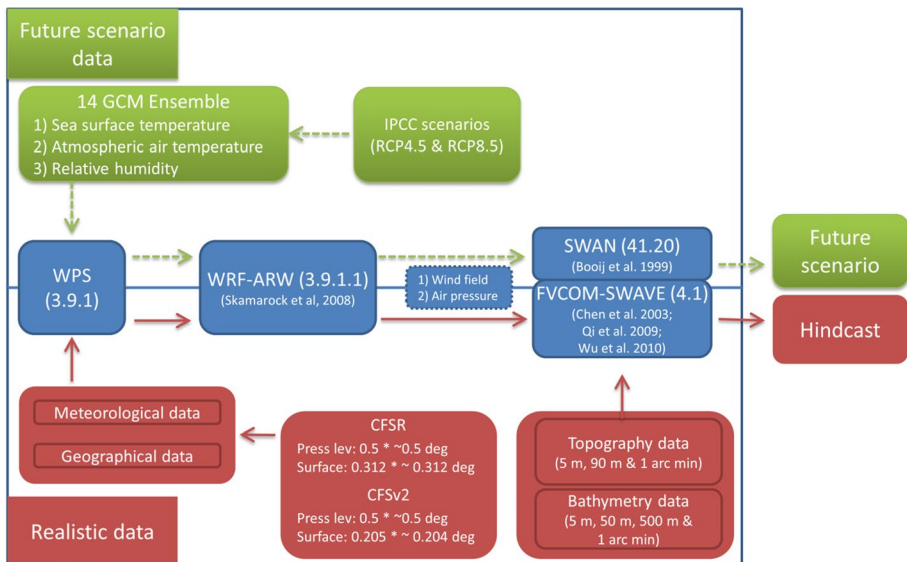


**Fig. 2** Flowchart of models used for hindcast and future simulations. The colour blue indicates the numerical models, red indicates various datasets used to force the models, and green shows 3 parameters and scenarios used from 14 GCM models as an ensemble

used as homogenous initial and boundary condition settings as possible (Table 1). All the WRF physics, calculation time steps and resolutions were the same for all events. For storms approaching the Atlantic Ocean (2005, 2010 and 2013 events), fixed homogeneous domains were used (Fig. 3a) and for the 2008 snow storm, approaching from the SE Europe, a different domain configuration was employed (Fig. 3b). The models were forced with the NCEP's Climate Forecast System Reanalysis (CFSR) datasets in  $0.5^\circ \times 0.5^\circ$  and  $0.312^\circ \times \sim 0.312^\circ$  resolution for pressure levels and surface, respectively. The CFSR data extended until the end of 2010. Therefore, for the 2013 storm case NCEP's Climate Forecast System version 2 (CFSv2) was used, with  $0.5^\circ \times 0.5^\circ$  and  $0.205^\circ \times \sim 0.204^\circ$  resolution for pressure levels and surface, respectively. The simulation results (hindcast) were then validated against observed data (provided by the Estonian Environmental Agency; [www.ilmateenistus.ee](http://www.ilmateenistus.ee)) at Estonian weathers stations and tide gauges (Vilsandi, Kihnu, Ruhnu, Pärnu; Fig. 4). The main study parameters were precipitation, wind speed and direction. Wind fields were studied in depth for the storm surge related 2005 and 2013 cases. For wave height validation, observation data from two stations were retrieved from the website of the Finnish Meteorological Institute (<https://en.ilmatieteenlaitos.fi/download-observations#!/>). The stations equipped with Datawell Waveriders are located in the Northern Baltic Proper ( $59^\circ 15' N 21^\circ 00' E$ ) and Gulf of Finland ( $59^\circ 58' N 25^\circ 14' E$ ; Fig. 4).

Furthermore, precipitation amount and spatial distribution comparisons were conducted for all the cases, with main incentive to see the precipitation spread and the differences between hindcast and future scenario simulations. The precipitations distribution maps were plotted as a total sum of convective (cumulus scheme) and non-convective (physics scheme) values at each grid point.

The wind field and pressure values from fine resolution (0.8 km) WRF domain 3 were used to force the FVCOM-SWAVE model in two storms (2005 and 2013) that caused a storm surge in the Pärnu city. The FVCOM-SWAVE computational domain was primarily designed to correctly simulate storm surges in the Gulf of Riga and particularly in the Pärnu Bay, which is the most vulnerable and surge-prone area in Estonia (Tõnisson et al. 2019). Therefore, fine bathymetric resolution (50 m) was used in the Gulf and even 5 m in the Pärnu Bay. As a computational trade-off, the high-resolution domains (both FVCOM-SWAVE and WRF d03) are not large. It encompasses the Gulf of Riga (surface area 18 100 km<sup>2</sup>) and just the most adjacent areas in the Baltic Proper (which bears no study interest here). Use of such a small domain for storm surge simulations at Pärnu is, however, justified because of semi-enclosed nature of the Gulf of Riga (Fig. 4). Large waves from the Baltic Proper do not propagate through the relatively narrow and shallow Irbe Strait into the Gulf of Riga. For rapid hydrodynamic response during ETCs the Gulf forms a specific, nearly enclosed sub-basin (Suursaar et al. 2002, 2006). However, influx of water through the open boundaries of FVCOM-SWAVE is still permitted.

Simulations were conducted for hindcast, RCP4.5 and RCP8.5 scenario studies. The FVCOM-SWAVE modelling domain (Fig. 4) used the same bathymetry and topography data as in Mäll et al. (2017). The main reasoning for using the same modelling domain was output quality allowing accurate results in simulating the storm surge at Pärnu city ( $-2.2\%$  peak bias compared to observations). The SWAVE component in the model is essentially a SWAN wave model (Booij et al. 1999) on unstructured grids and coupled with FVCOM through radiation stress, bottom boundary layer and surface stress (Qi et al. 2009; Sun et al. 2013). The study by Mäll et al. (2017) used air-sea drag coefficient proposed by Honda–Mitsuyasu (1980), as opposed to default coefficient used in FVCOM. In this study, the authors, however, considered the coefficient proposed by Wu (1982) with upper

**Table 1** Initial and boundary conditions of the models

WRF	2005	2008	2010	2013
Domain 1 (res. 20 km)	01/06 00:00–01/10 12:00 (108 h)	11/19 18:00–11/26 00:00 (150 h)	02/26 00:00–03/03 18:00 (138 h)	10/26 00:00–10/31 00:00 (120 h)
Domain 2 (res. 4 km)	01/07 06:00–01/10 12:00 (78 h)	11/20 06:00–11/25 12:00 (126 h)	02/28 12:00–03/03 18:00 (78 h)	10/27 12:00–10/31 00:00 (84 h)
Domain 3 (res. 0.8 km)	01/08 06:00–01/10 12:00 (54 h)	11/21 12:00–11/25 06:00 (90 h)	03/01 12:00–03/03 18:00 (54 h)	10/28 06:00–10/30 12:00 (54 h)
Time step	d01—120 s, d02—24 s, d03—4.8 s			
Map projection	Lambert conformal			
Pressure top, vertical layers	1 hPa; 61			
Micro physics	WRF Single-moment 6-class scheme (Hong and Lim 2006)			
Planetary boundary layer	Yonsei University Scheme; YSU (Hong et al. 2006)			
Cumulus parameterization	Grell-Freitas Ensemble Scheme (Grell and Freitas 2014)			
Shortwave and longwave	RRTMG Shortwave and Longwave Schemes (Iacono et al. 2008)			
Land surface option	Unified Noah Land Surface model (Tewari et al. 2004)			
Surface layer option	Revised MM5 Scheme (Jimenez et al. 2012)			
Forcing data	Climate Forecast System Reanalysis (CFSR)			CFSv2
Forcing data res	Pressure levels (1): 0.5 * 0.5° Surface (2): 0.312 * ~0.312°			(1): 0.5 * 0.5 (2): 0.205 * ~0.204°
FVCOM-SWAVE	2005			2013
Simulation time	01/08 06:00–01/10 12:00 (54 h)			10/28 06:00–10/30 12:00 (54 h)
Calculation time step	Sea level—2 s; significant wave height—30 s			
Nodes	63 189			
Cells	123 533			
Mesh size	50–2000 m			
Coastline data	Pärnu City—5 m (DEM LIDAR); Pärnu Bay—90 m (SRTM90); rest of the study area—1 arc min (ETOPO1)			
Bathymetry data	Pärnu Bay and Pärnu River—5 m (EMA); Gulf of Riga, Väinameri and Irbe Strait—50 m (EMA); rest of the study area 1 arc min (ETOPO1)			
SWAN/SWAVE	2005			2013
Frequency range (Hz)	0.05–0.5			

**Table 1** (continued)

SWAN/SWAVE	2005	2013
Direction	Full circle	
Bottom friction	Madsen formulation (Madsen et al. 1988)	
Friction parameter	0.067	
Min water depth (m)	0.05	
SWAN bathymetry	500 m (BSBD v0.9.3)	
SWAN simulation time	01/07 06:00–01/10 12:00 (78 h)	10/27 12:00–10/31 00:00 (84 h)

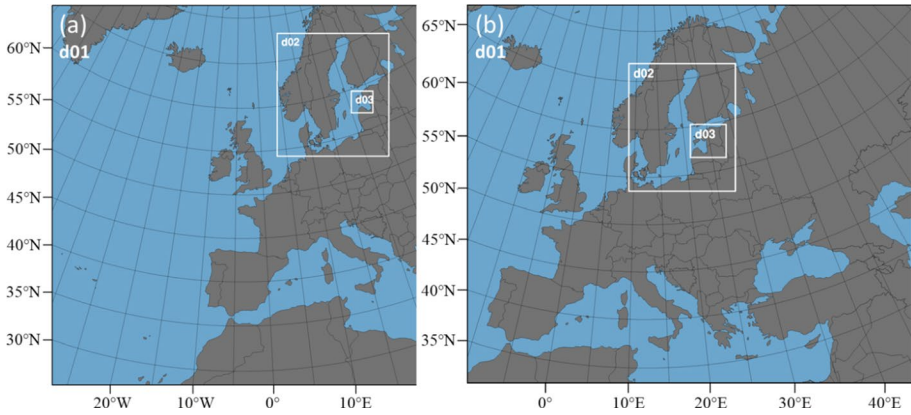


**Fig. 3** WRF modelling domains (d01, d02, d03) for 2005, 2010 and 2013 case studies (a), and for the 2008 case study (b). D03 also corresponds to FVCOM-SWAVE domain, and d02 encompasses the SWAN domain inside the Baltic Sea (for 2005 and 2013 case studies)

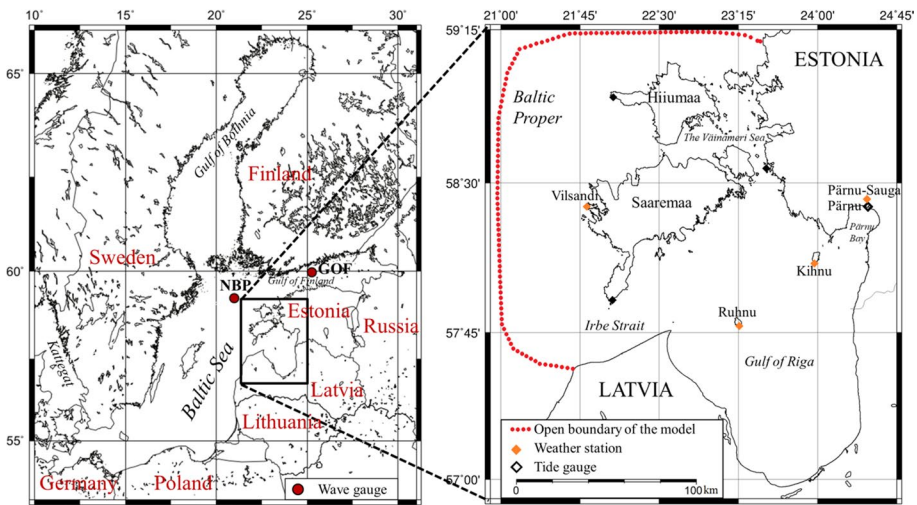


**Fig. 4** Area map of the Baltic Sea with its surrounding countries is shown on the left, which also represents the SWAN modelling domain. The wave gauges are marked NPB (Northern Baltic Proper) and GOF (Gulf of Finland). The modelling domain (same as d03 in WRF) of FVCOM-SWAVE model with validation locations is shown on the right

limitation of 0.003. Among the three coefficients, this yielded the most accurate results in the study area. The parameter selections for FVCOM-SWAVE can be seen in Table 1.

## 2.2 CMIP5 model data and future scenarios

In this study, 14 general circulation models (GCMs) were considered for future scenario calculations. The main selection criteria were based on the study by Zappa et al. (2013a), which suggested that among current CMIP5 GCMs, high-resolution set-up (~T106/N96)

might be needed to better capture the extratropical North Atlantic storm track in winter months. Another necessary criteria was that all the GCMs need to have RCP4.5 and RCP8.5 projection (IPCC 2014) data available for years 2081–2100 (hereafter “2090”) and have experiment data on AAT, SST and specific humidity (converted to RH). An exception was made for HadGEM2-CC model, which data extends from 2081 to 2098, however met other set parameters. Accordingly, 14 GCMs were considered for the current study (Table 2) and their data was downloaded from The Earth System Grid Federations website (<https://esgf-node.llnl.gov>). The authors did not perform any specific bias corrections for the downloaded raw GCM output data. The pseudo-climate framework employed the storyline approach (e.g. Hazeleger et al. 2015; Maraun et al. 2017), working with specific climate differences calculated between the “present” and “future” conditions in the ensemble of 14 GCMs, and did not study the absolute dynamics of the projections.

Multi-model ensemble mean was calculated based on the 14 GCMs for each event month and future scenario. The GCM data was monthly averaged; therefore, each of the four storm months corresponded to specific months extracted from GCMs. For example, the 2005 storm occurred in January; therefore, only January values were used for this storm (and similarly, 2008 November, 2010 February, and 2013 October). The data for each month was divided into two groups—control period (CP) and future period (FP). The CP corresponded to monthly average values between 2006 and 2015, and the FP corresponded to data from 2081 to 2100 (with the exception of HadGEM2-CC). The FP and CP differences were then calculated and interpolated onto meteorological grids (created with the WRF pre-processing system, WPS), thus producing new initial conditions for the WRF simulations.

### 3 Storm review

#### 3.1 Gudrun (2005)

The winter storm Gudrun, also known as Erwin in the British Isles and Central Europe, developed south of Newfoundland as a gradually deepening low pressure system of the polar front on 6 January 2005. It passed over Scotland and Scandinavian Peninsula and reached the Baltic Sea on 8–9 January 2005. The nadir point of 959 hPa was achieved near Oslo at 15:00 UTC on 8 January 2005 (Post and Kōuts 2014). According to the Danish Meteorological Institute (DMI), the highest sustained wind speeds reached  $35 \text{ m s}^{-1}$  and gusts  $46 \text{ m s}^{-1}$  in Denmark. Portions of Estonian territory also fell into the zone of the cyclone’s strongest jet winds on the right-hand side of the track. Maximum hourly average speeds of SW and W winds reached  $28 \text{ m s}^{-1}$  on the western Estonian coast, and gust wind speeds reached  $38 \text{ m s}^{-1}$  at Kihnu (Suursaar et al. 2006). Actual maximum wind speeds could have been somewhat stronger as disruptions in measurement left gaps in several wind speed records just beside the highest archived values. Also there was missing or distorted data from some of the tide gauges.

The average Baltic Sea level had already been high since December 2004 as a result of preceding cyclones and persistent westerlies that forced the water from the North Sea into the Baltic basin (Fig. 5). During Gudrun, the new highest sea levels were recorded in many locations along the western Estonian coast (Suursaar et al. 2006), as well in Finland (Averkiev and Klevanny 2010). At Pärnu, the sea level height reached 275 cm over the long-term mean in Baltic Height System 1977 (BHS77; see also Suursaar and Kall 2018),



**Table 2** List of CMIP5 models including resolution and ensemble information

ID	Model name	Model institution	Atmospheric resolution		Ensemble number	Ensemble name
			Horizontal	Vertical levels		
G1	ACCESS1.0	Commonwealth Scientific and Industrial Research Organization (CSIRO) and Bureau of Meteorology (BOM), Australia	192 × 145 (N96)	38	1	r1i1p1
G2	ACCESS1.3				1	r1i1p1
G3	BCC-CSM1.1 (m)	Beijing Climate Center, China Meteorological Administration	T106	26	1	r1i1p1
G4	CCSM4	National Centre for Atmospheric Research	0.9° × 1.25°	27	6	r1i1p1, r2i1p1, r3i1p1, r4i1p1, r5i1p1, r6i1p1
G5	CESM1(BGC)	NFS-DOE-NCAR	0.9° × 1.25°	27	1	r1i1p1
G6	CESM1(CAM5)				3	r1i1p1, r2i1p1, r3i1p1
G7	CMCC-CM	Centre Euro-Mediterraneo per I Cambiamenti Climatici	0.75 × 0.75 (T159)	31	1	r1i1p1
G8	EC-EARTH	EC-EARTH consortium	1.125 long, Spacing, T159L62	62	4	r1i1p1, r6i1p1, r8i1p1, r12i1p1
G9	GISS-E2-H-CC	NASA Goddard Institute for Space Studies	Nominally 1°	40	1	r1i1p1
G10	GISS-E2-R-CC				1	r1i1p1
G11	HadGEM2-AO	National Institute of Meteorological Research/Korea Meteorological Administration	1.875 long × 1.25 lat (N96)	60	1	r1i1p1
G12	HadGEM2-CC	UK Met Office Hadley Centre (additional HadGEM2-ES realizations contributed by Instituto Nacional de Pesquisas Espaciais)	1.875 long × 1.25 lat (N96)	60	3	r1i1p1, r2i1p1, r3i1p1
G13	HadGEM2-ES				4	r1i1p1, r2i1p1, r3i1p1, r4i1p1
G14	MRI-CGCM3	Meteorological Research Institute	320 × 160 (TL159)	48	1	r1i1p1

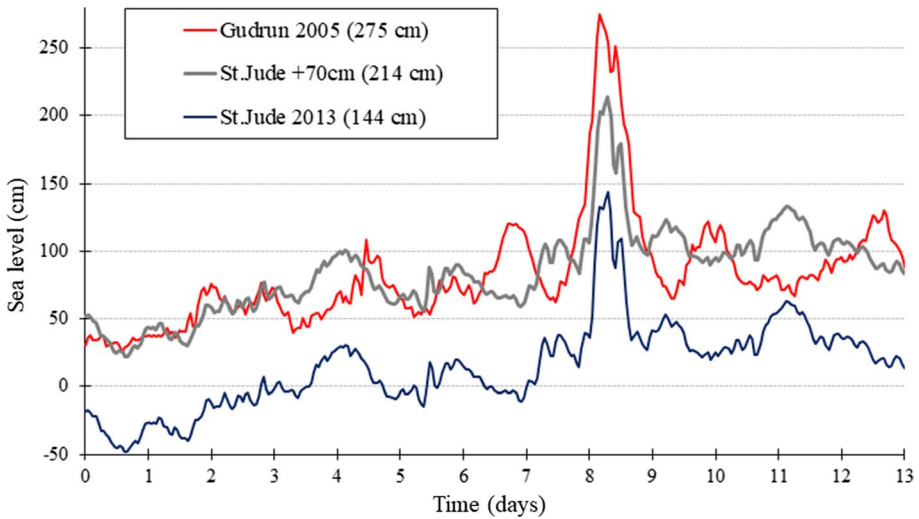


**Fig. 5** Comparison on sea level variations at Pärnu during Gudrun and St. Jude storm. Gudrun time starts 1 January 2005 (00:00 UTC), St. Jude time starts 21 October 2013 (00:00 UTC); Zero sea level—BHS77 zero; Pärnu average was 1.5 cm in 1924–2016, and 0.0 cm in 1924–1985

of which the surge component constituted approximately 190 cm. The non-tidal 12 h sea level gain reached 188 cm. Although nearly 32% of households lost power in entire Estonia, the main damage during Gudrun occurred as a result of flooding of the urban areas. As the previous highest surge (253 cm) took place nearly 38 years earlier (on 18 October 1967), the scale and consequences of the new flooding were quite unexpected both for the population and authorities (Tönisson et al. 2019).

### 3.2 St. Jude (2013)

Prolonged stormy period above northern Europe began in October 2013 and lasted until the middle of January 2014. Originated at the polar front in the region south of Iceland, a series of extratropical cyclones (including St. Jude, Hilde, Xavier and some others) crossed the Baltic Sea from west to east. The first in this series was the St. Jude storm, known also as Cyclone Christian (in Germany), Carmen (in UK) or Allan (in Denmark). Forming on the 26 October, the atmospheric depression travelled eastward. Quite similarly to storm Gudrun, the cyclone continued across the North and Baltic Sea (Fig. 1). The record-breaking gust-wind speeds were recorded both in Netherlands (up to  $41 \text{ m s}^{-1}$ ) and Denmark (up to  $53 \text{ m s}^{-1}$ ). In Estonia, the strongest recorded 1 h-sustained wind speeds (from SW-W) were  $22.1 \text{ m s}^{-1}$  at Sõrve and  $23.2 \text{ m s}^{-1}$  at Roomassaare on 29 October. The gust wind speeds reached  $32 \text{ m s}^{-1}$ .

The cyclone also caused a storm surge and high waves in the eastern Baltic Sea (Viitak et al. 2016). At Pärnu tide gauge, the maximum sea level of 144 cm was recorded at 07:00 UTC on 29 October (Fig. 5). At Narva, within 10 h the sea level rose from the initial -21 cm to the final 132 cm at 10:00 UTC. The sea level heights remained relatively modest only because St. Jude was the first cyclone of the season and the background sea level of the Baltic Sea was not elevated yet (in fact, it was even below long-term

mean). If the Baltic background sea level would have been similar to that of Gudrun (Fig. 5), the Pärnu maximum sea level could have been 214 cm, which is well over the 160 cm critical value and ranking third (after 275 cm in 2005 and 253 cm in 1967) since the beginning of the measurements in 1923 (Jaagus and Suursaar 2013; Suursaar et al. 2015).

### 3.3 November storm (2008)

The storm affected Estonia, Finland, and Russia’s Pskov and Leningrad oblasts. It started to develop near the Black Sea area on 21 November and approached Estonia from the southeast by 23 November (Fig. 1). At first, an undulating upper-tropospheric jet stream extended southward to the Mediterranean Sea, allowing cold air-masses to spread south, and warm moist air towards north on its eastern side. The wave-like structure developed into a closed circulation and formed a cyclone at surface, which shifted northwards. According to meteorological analysis (Nevalainen 2012), the cyclone deepened with a “bomb” rate (more than 12 hPa in 12 h, according to Sanders and Gyakum, 1980) and probably reached 952 hPa. Until the cyclone occluded above Finland on 24 November, it brought heavy winds and 24 h snowfall accumulation of up to 33 cm at Helsinki, Southern Finland. It caused power cuts in 41,000 households in Finland alone, numerous traffic accidents and damage to buildings (Rauhala and Juga 2010).

According to Estonian data, the lowest atmospheric pressure (951–952 at several stations) was measured on 23 November (20:00 UTC), the 24 h deepening rate being 36.8 hPa and a 12 h drop of 23.0 hPa. Wind direction rotated counter-clockwise from W to S and E (22 Nov.), and finally to N (23 Nov.; Fig. 6a). Bringing cold air, the northerlies reached 16–18 m s<sup>-1</sup> (as 1 h averages), while maximum gusts reached 30 m s<sup>-1</sup> at Pakri (Fig. 6a). The heaviest snowfall was associated with northerlies during 23–24 November. The depth of the snow-cover reached 30–50 cm in most of the Estonia’s continental stations (Fig. 6b). Although the precipitation amount was everywhere

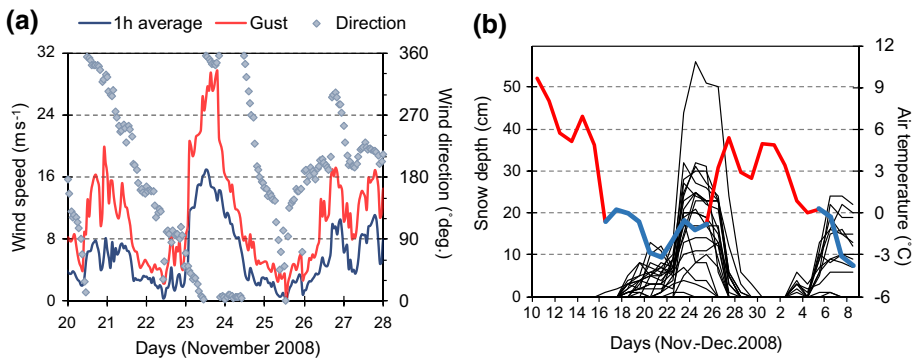


**Fig. 6** **a** Variations in hourly average wind speeds, directions and maximum gusts at Pakri station during the November 2008 snowstorm. During the cyclone, wind direction rotates from east to north (bringing cold air) and later on to west (for warmer air). **b** Variations in snow cover depth at 21 Estonian meteorological stations (non-specified thin black lines; maximum 56 cm was measured at Kuusiku on 25 Nov. 2008). Daily average air temperatures at Türi (near Kuusiku) showing positive (red) and sub-zero (blue) temperatures

considerable, in West Estonia it partially fell down in liquid form, thus not adding much to snow-cover.

### 3.4 Xynthia (2010)

Xynthia was the severest European windstorm in 2010, which crossed Western Europe between 27 February and 1 March 2010, causing 64 reported casualties (Liberato et al. 2013). It was generated close to Madeira Islands, from there it moved across to the Canary Islands, Portugal, northern Spain and south-western France (Fig. 1). The highest gust wind speeds reached  $44 \text{ m s}^{-1}$  in France. Although the minimum sea level pressure was 965 hPa, the storm impacts included storm surge and rough seas hitting coastal regions of France at high tide (Bertin et al. 2012), as well as river floods in France, Spain, Switzerland and Germany.

Being considerably weakened by that time, the storm reached the Baltic Sea from southwest on 1–2 March 2010. It was detectable in Estonia by moderately low (980–990 hPa; Fig. 7a) atmospheric pressure and fresh wind conditions (1 h average wind speeds  $11\text{--}12 \text{ m s}^{-1}$  at coastal stations, max. gusts up to  $17 \text{ m s}^{-1}$ ; Fig. 7b). The cyclone also brought warm ( $+2 \text{ }^\circ\text{C}$ ) and moist air from south, and the wind direction abruptly changed from SE to NW, as the center of the cyclone crossed Estonia. Even if its impacts as an occluding depression were not noteworthy in Estonia's context, it still was an interesting case due to its long course and preceding history. An interesting question is, would the storm retain its strength further north in future climates?

## 4 Modelling results and discussion

The performance of the modelling system was validated using partly different aspects of each storm. Once the model performance was on adequate level, it was not necessary to compare (validate) all the possible output data. Strictly speaking, the study does not analyse the future (year 2081–2100) simulation results in comparison with the past measurements, but past and future simulations obtained with the same model. The current section

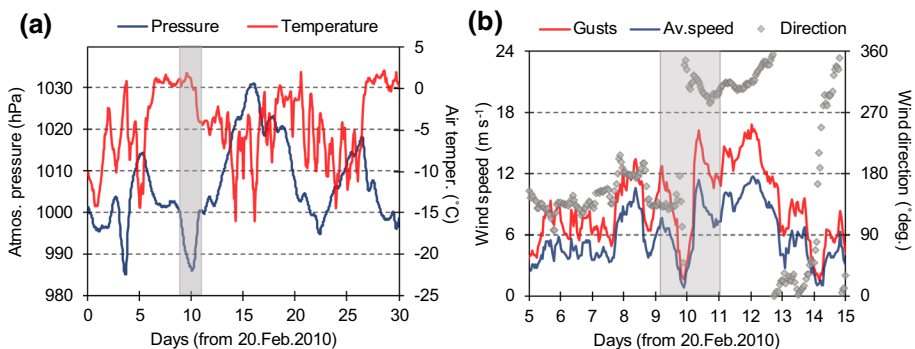
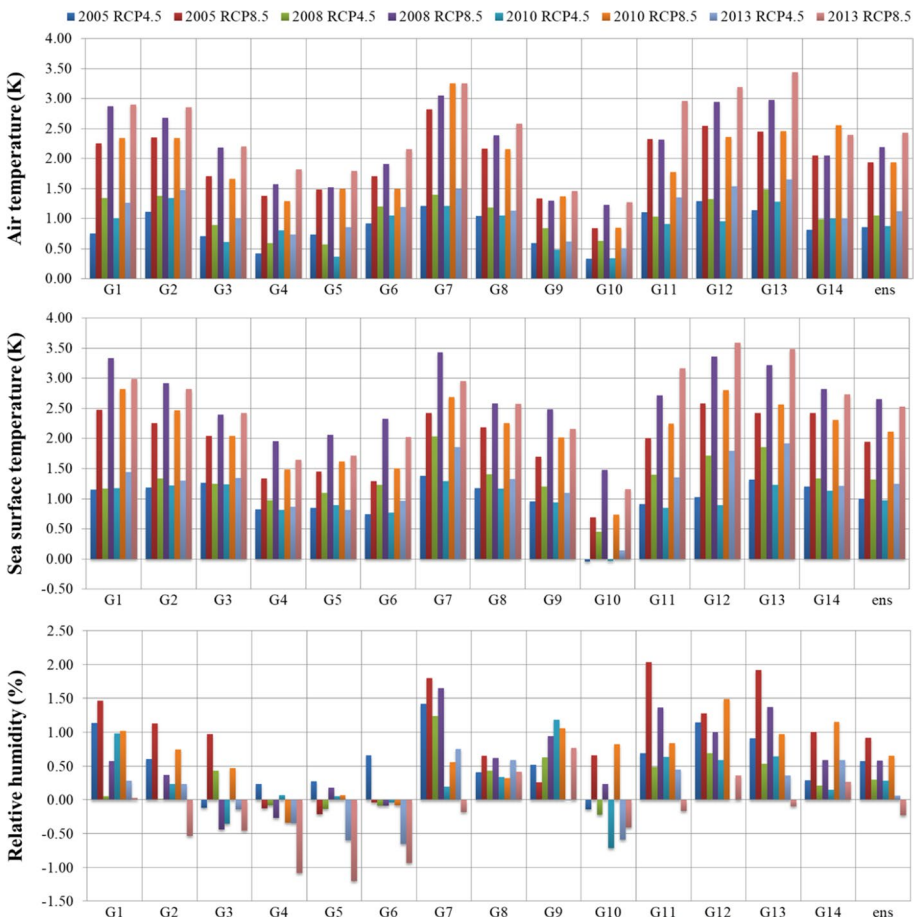


**Fig. 7** **a** Variations in hourly atmospheric pressure and air temperature at Kihnu station during the 2010 storm. Approaching Xynthia (1–2 March is marked by grey area) brought warm air from south to Estonia. **b** Variations in wind speed and direction at Vilsandi. The centre of the weakened cyclone crossed West Estonia, causing the abrupt wind direction change (SE→NW)

is divided into three main subsections: (1) description and analysis of CMIP5 output, (2) analysis of wind, wave plus surge simulations and (3) precipitation simulations. The hind-cast and future scenario calculations are presented and discussed conjointly.

### 4.1 CMIP5 GCM analysis

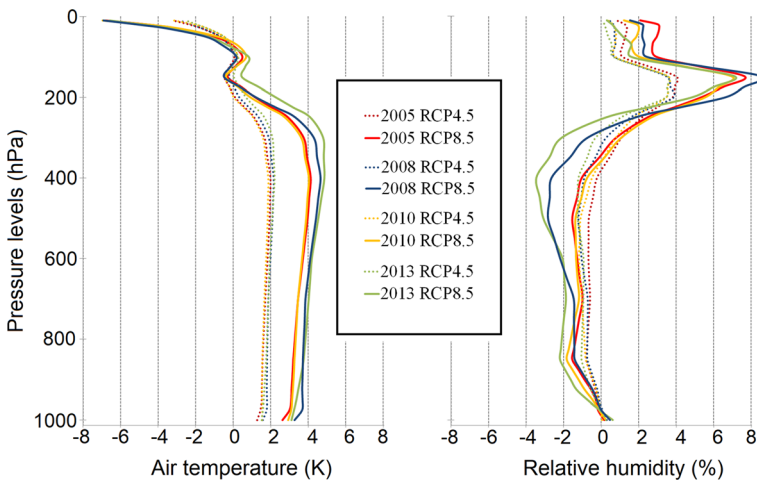
An essential part in understanding how the studied extreme weather events might change under potential climate change conditions, is to know to what degree the initial conditions would change. The previous study by Mäll et al. (2017) used data from a single GCM, the MIROC5 (not included in this study). However, using a single GCM output comes with an inherent bias factor to it, as the various GCM outputs tend to vary greatly (Fig. 8; Table 3). Therefore, it would be necessary to use multi-model ensemble in order to reduce a degree of uncertainty (e.g. Pinto et al. 2011) and to assess variability between individual model outputs.



**Fig. 8** Projected changes from all the 14 GCMs for AAT, SST and RH (see Table 2 for model reference and Table 3 for statistics)

**Table 3** Averages (Av.), standard deviations (SD) and coefficients of variance (CV) of all 14 GCM models for AAT ( $^{\circ}$ K), SST ( $^{\circ}$ K) and RH (%) over the WRF domain 1

		AAT			SST			RH		
		Av	SD	CV(%)	Av	SD	CV(%)	Av	SD	CV(%)
2005RCP4.5	January	0.86	0.30	35	0.99	0.36	36	0.58	0.47	81
2008RCP4.5	November	1.06	0.32	30	1.31	0.39	30	0.30	0.41	137
2010RCP4.5	February	0.88	0.32	36	0.97	0.34	35	0.29	0.50	172
2013RCP4.5	October	1.13	0.36	32	1.24	0.47	38	0.07	0.48	686
2005RCP8.5	January	1.95	0.56	29	1.95	0.57	29	0.92	0.75	81
2008RCP8.5	November	2.21	0.64	29	2.64	0.58	22	0.58	0.63	109
2010RCP8.5	February	1.95	0.64	33	2.11	0.60	28	0.65	0.51	78
2013RCP8.5	October	2.45	0.69	28	2.53	0.72	28	-0.23	0.59	256

**Fig. 9** Horizontally averaged AAT and RH differences over the WRF parent domain

A comparative analysis for all the future scenarios (8 in total) included horizontally averaged pressure levels of AAT and RH. Since all the considered storms occurred under diverse thermal conditions, the vertical distributions based on the ensemble mean also differed to an extent. For AAT, the RCP4.5 and RCP8.5 differences were more apparent, where the RCP8.5 values were almost  $2^{\circ}$ K higher compared to RCP4.5 (Fig. 9). At around 250 hPa height (about 11 km), the differences started to decrease, and turned into decrease in stratospheric heights. Highest increase occurred in 2013RCP8.5 (October month) and in 2008RCP8.5 (November), respectively. Roughly similar vertical tendencies occurred in the RCP4.5 scenarios as well.

The mean SST rise relative to the CP (2006–2015) showed larger changes in the RCP8.5 case (Fig. 10), and similar in increase to that of the AAT cases (Fig. 9; Table 3). For RCP4.5, the SST extremes were rather modest when compared to RCP8.5. All scenarios exhibited similar patterns in change, where the semi-enclosed water bodies (e.g. the Baltic Sea and Mediterranean Sea, also the Norwegian Sea) showed the highest increases. The SST differences became less apparent or even slightly negative (2005 and 2010 scenarios)



in the North Atlantic, SW from Iceland. This negative tendency was more pronounced for the months January and February. Overall, the most pronounced changes occurred in October and November.

Compared to RCP4.5, the overall parameter changes in RCP8.5 were more pronounced, and also more reliable, as estimated on the basis of coefficients of variation (CV, calculated as  $SD/Av.$  ratio and presented as percentages) among the 14 CMIP5 model output values (Table 3). For instance, the CVs were smaller in RCP8.5 calculations than in RCP4.5 (e.g. 22–28% vs. 30–38% in SST). The same basically applied for AAT and RH as well. On the other hand, the RH changes were least reliable due to relatively high SDs (and thus, CVs).

## 4.2 Metocean results for 2005 storm Gudrun

The hindcast modelling results for the 2005 storm Gudrun were slightly different when compared to previous study by Mäll et al. (2017). The differences were probably attributed to changes made in initial and boundary conditions and use of 14 model ensemble. In the current study, higher horizontal and vertical resolutions were applied, and the domain 1 and 2 sizes have been increased. In particular, the increase in domain sizes influenced greatly the accuracy of local wind values (smaller domains yielded better results). The main argument for using larger domains and therefore accepting somewhat decreased accuracy was that larger parent domains allow better to capture the changes in cyclogenesis processes invoked by the new calculation conditions. Furthermore, for the sake of homogeneity, the single-domain set-up for Atlantic storms needed to encompass all the locations where the three storms originated from.

Although a backward shift in the wind speed peak timing for the Kihnu and Ruhnu stations was observed (Fig. 11), the maximum values were captured with good accuracy. Results for Vilsandi and Pärnu-Sauga stations showed the best fit with the observed values. The drop in observed wind speed at Vilsandi station occurred due to the stations proximity to a lighthouse, which dampened the wind measurements from 210° to 250° sector.

Concurrently to the results at Kihnu and Ruhnu station locations, which possesses the largest potential for evoking storm surge in Pärnu Bay (Fig. 11), the simulated FVCOM-SWAVE results showed higher initial increase in the sea level and reached its first peak maximum of 2.41 m at 9 January 00:20 UTC (observed was 2.75 m at 9 January 04:00 UTC). The almost 4 h difference can be attributed to the wind field quality which also reached its first peak maximum 3 h before the observed measurements.

The future simulations, on the other hand, showed more pronounced outcome, compared to the previous study, where no increase in intensity was observed. At Kihnu station (closest to Pärnu Bay; Fig. 4), the peak hourly sustained wind values under RCP4.5 and hindcast conditions reached 25.5 and 25.0  $m s^{-1}$ , respectively. This difference also translated into surge height increment (Fig. 11; Table 4), yielding in maximum surge values of 3.0 m for RCP8.5 and 2.59 m for RCP4.5, as opposed to 2.41 m in hindcast simulation. Hence, the peak surge height increased 19.7% under RCP8.5, while under RCP4.5 the increase was 7%. Considering the scatter among the individual model outputs (Table 3), the increase in RCP4.5 was not significant, but it was under RCP8.5.

Since the RCP8.5 case showed significant station-based changes (Fig. 11), the authors also compared hindcast and RCP8.5 simulations on a regional scale (WRF domain 2) to see whether there were any significant changes in cyclone track and/or wind field (Fig. 12). In terms of pressure field, the RCP8.5 had an equal or slightly higher (by up to 2 hPa)

**Fig. 10** SST spatial distribution changes among all the future scenario calculations with indicated average SST differences (°K) over the corresponding domain by year 2090 relative to CP. The light blue still marks temperature rise; GCM data did not include information on inland water bodies. Note that the d01 coverage for the southerly 2008 November storm is different from the others (see Fig. 3)

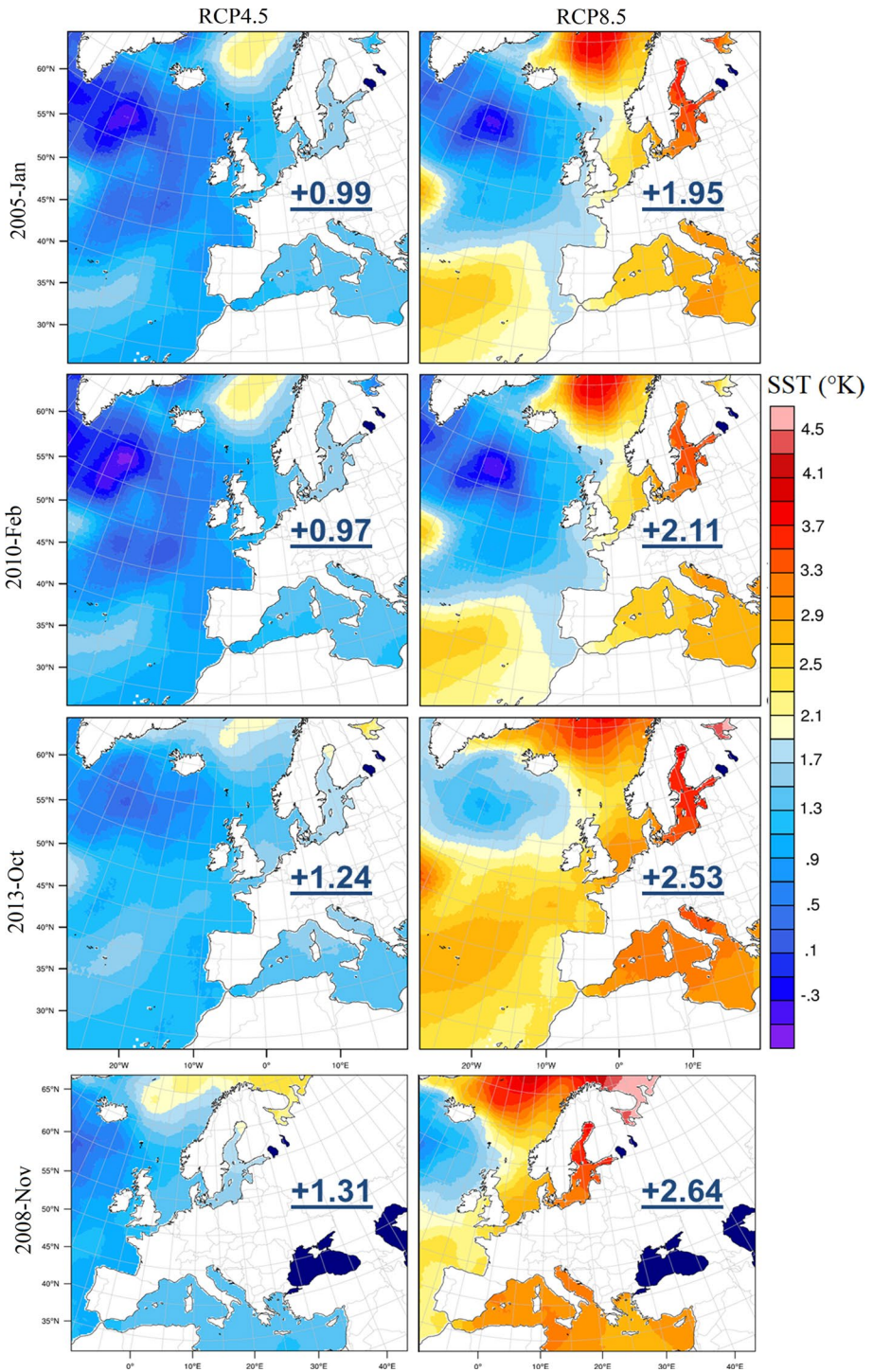
minimum sea level pressure (MSLP) values at the cyclone core, compared to the hindcast. However, the MSLP area of RCP8.5 was more symmetrical compared to hindcast and thus covering somewhat larger area. This, in turn, could strengthen pressure gradient on the southern side of the cyclones core (due to more densely packed isobars; Fig. 12), and hence, also local winds. The extent of high wind speed field ( $\geq 24 \text{ m s}^{-1}$ ) stretched farther southwards from the core boundary. Stronger winds extensively occurred over Baltic Proper, Gulf of Riga and Danish straits.

The hindcast simulation results for wind waves at the station which has the longest fetch area (Northern Baltic Proper; NBP) generally showed good agreement with the observed significant wave height values (Fig. 13). However, the peak heights were overestimated by 1.2 m (7.2 m observed vs. 8.4 m simulation). Similar model overestimations for the NBP were forecasted by various meteorological institutes at the time of the event, as discussed and presented by Soomere et al. (2008). In fact, our modelling results were very close to those forecasts (by DMI, DWD and FIMR; Soomere et al. 2008; Fig. 13). While the measurements and hindcasts generally behave similarly in “normal” conditions, during the peak wave conditions either the models are overestimating or the Waverider underestimating the actual wave heights. It is possible that the Waverider measurements were, in some reason, not quite representative during the peaks of the extreme storms. In particular, the measured wave heights around 3 m in the Gulf of Finland seems to be much too low for such an extreme storm (Fig. 13), while 5.2 m  $H_s$  has been attained several times, before and after the 2005 storm (Björkqvist et al. 2018). Gulf of Finland comparison could suffer from measurement gaps during the storms, due to specific configuration of the Baltic Sea and narrow fetch geometry of the Gulf of Finland itself (Björkqvist et al. 2018).

Compared to hindcast, the future simulations showed no significant change in  $H_s$  maximums at either station locations. However, under RCP8.5 the calculated wave field patterns showed a notable southward extension of the high wave zone, increase in maxima within the Baltic Proper (9.2 m vs 8.7 m; Fig. 14), and also in the Gulf of Riga. This was related to the south-ward extension of stronger wind fields as shown in Fig. 12.

### 4.3 Metocean results for 2013 storm St. Jude

The analysis section for Gudrun explained how configuring simulation conditions can affect the simulation accuracy. In the 2013 storm case, on the other hand, simulated wind speed curves at the four stations showed a remarkably good fit with the observed values (Fig. 15). The peak wind speed values and their timings were well captured, showing no significant deviations. Also the wind speed values before and after the peak were more concurrent with observations. The observed drop in Vilsandi was caused by the same reason as for the 2005 case (lighthouse shade). The observed surge peak at Pärnu was 1.44 m (29 Oct. 07:00 UTC). The FVCOM-SWAVE hindcast simulation peak maximum was 1.19 m (29 Oct. 04:00 UTC). Furthermore, in both 2005 and 2013 cases, the observed second peak at Pärnu was caused by the 5 h seiche period of the Gulf of Riga sub-basin (Suursaar et al. 2002). In terms of relationship between surge potential and wind direction, Pärnu Bay is most susceptible to winds from  $220^\circ$  (Suursaar et al. 2006). The 9-h average wind



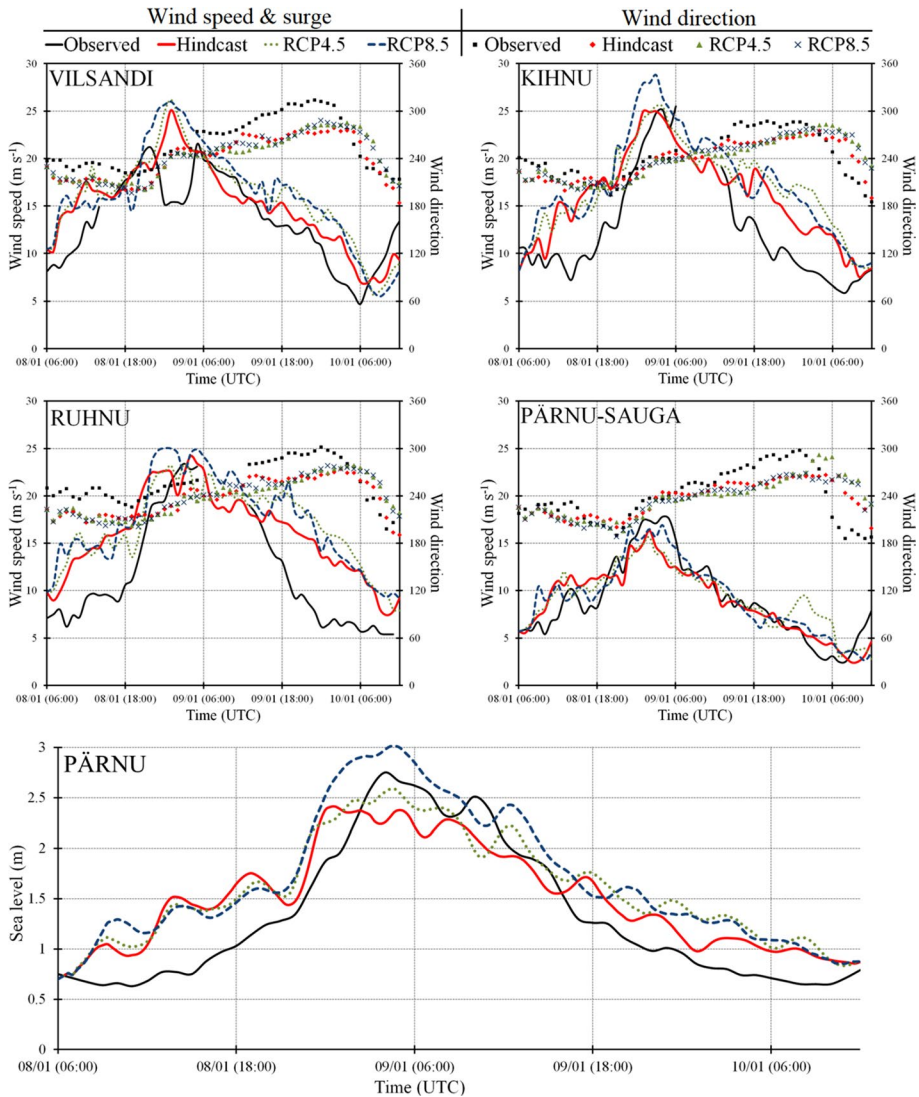


**Fig. 11** Modelling results for the 2005 storm Gudrun. The upper two rows show wind speed and direction at selected stations, and the bottom image shows the surge results at Pärnu (see also Fig. 4)

**Table 4** Maximum surge heights and surge increments (relative to hindcast) in different scenarios by ~2090

Scenario	Max. (cm)	Increment (%)
RCP4.5 Gudrun	259	6.9
RCP4.5 St. Jude	122	2.5
RCP8.5 Gudrun	301	19.9
RCP8.5 St. Jude	142	16.2



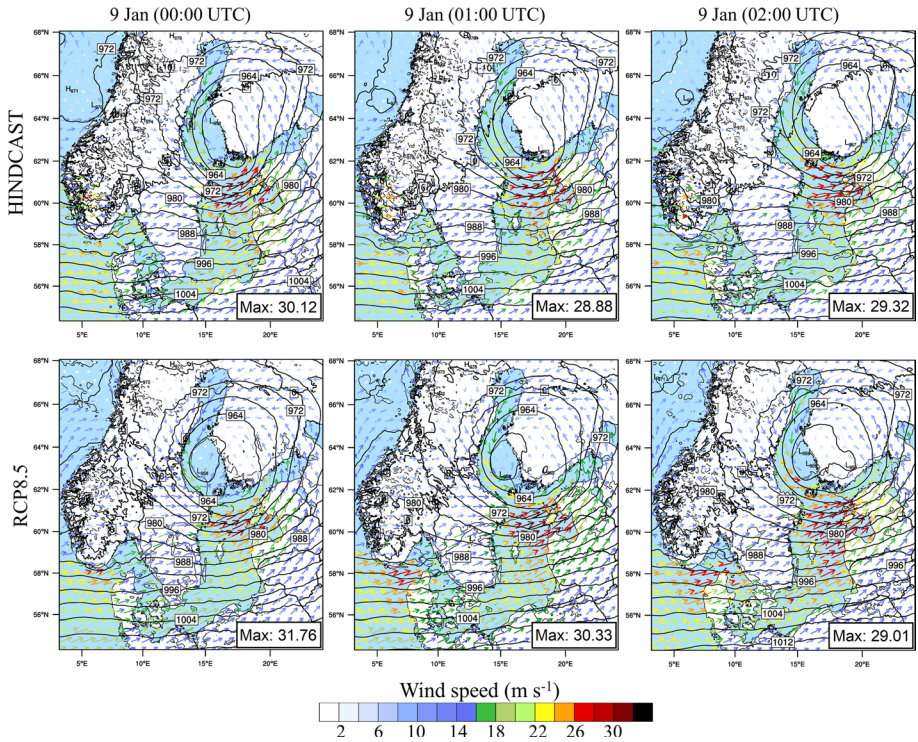


**Fig. 12** Wind and MSLP fields over WRF d02 for hindcast and RCP8.5 simulations (2005 case). The “Max” values indicate maximum hourly wind speed values at a given time-step

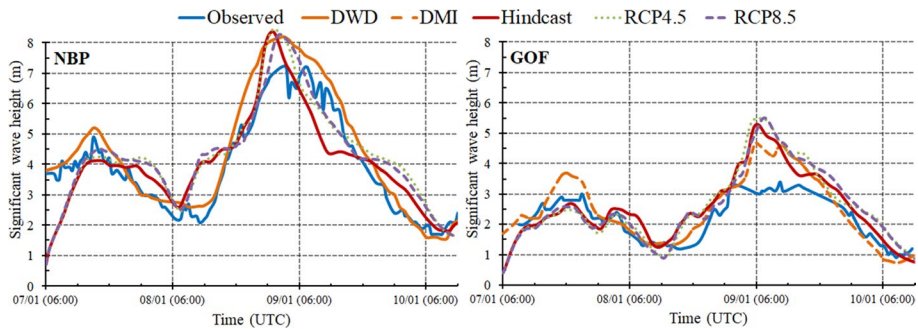


**Fig. 13** SWAN simulation and observed significant wave height comparisons at the two wave gauge stations (see also Fig. 4). The Deutscher Wetterdienst (DWD) and DMI data were reproduced from Soomere et al. (2008)

directions at Ruhnu station were 210° and 226° for hindcast and observations, respectively (Fig. 15). At Kihnu, the hindcast wind directions were close to the most suitable 220° mark as well.

Similarly to the 2005 case, future scenario calculations under RCP4.5 scenario had little to no increase in wind speed, while RCP8.5 showed clear increase over the Gulf of Riga

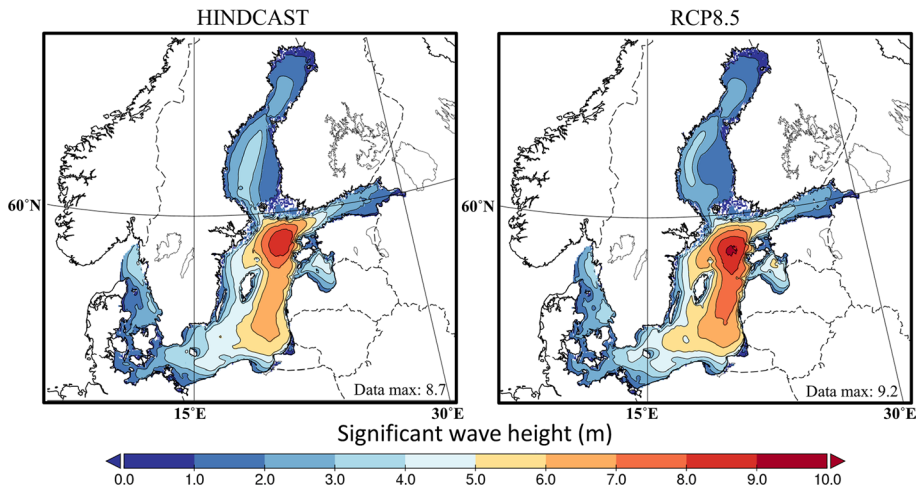


**Fig. 14** Spatial distribution of SWAN simulation results for the hindcast and RCP8.5 case at Jan-9 01:00 UTC, during the occurrence of highest simulated significant wave heights

(Fig. 15). Also a slight increase at peak value occurred at Vilsandi station. These higher wind speed values were also translated into higher storm surge simulation results (Fig. 15; Table 4). The peak differences for RCP8.5 wind speeds were 0.7, 1.6 and 1.0  $\text{m s}^{-1}$  for Vilsandi, Ruhnu and Kihnu stations, respectively. The changes, especially at Kihnu station, were not as profound as was for the 2005 case (3.8  $\text{m s}^{-1}$  increase at Kihnu for the 2005 RCP8.5). The RCP4.5 surge simulation yielded peak value of 1.22 m (just 0.03 m increase over the CP), while RCP8.5 surge simulation yielded 1.41 m (0.22 m or 15.6% increase). In physical point of view, it is difficult to explain the differences between outcomes for the 2005 and 2013 storms (Figs. 12, 16, Table 4). One can still hypothesize that, although approaching along fairly similar courses, the storms essentially belonged to different seasons (January and October), and thus, to different thermal and dynamical conditions.

The 2013 regional pressure field (Fig. 16; WRF domain 2) differences between hindcast and RCP8.5 had less apparent changes than during the 2005 storm. The core pressure levels stayed the same (968 hPa) for both hindcast and RCP8.5 throughout the investigated 4 h period. Furthermore, the central pressure area location, spread and pattern remained almost unchanged, with the more notable exception of slightly elongated isobars spread from the core. The maximum wind speed values also remain largely unchanged, with an exception where significant increase of 3  $\text{m s}^{-1}$  for the RCP8.5 at 29 October 05:00 UTC occurred. In terms of strong wind speed ( $\geq 22 \text{ m s}^{-1}$ ) spatial distribution, the RCP8.5 showed a slight southwards extension of stronger winds (therefore stronger winds over the Gulf of Riga) which seemed to be related to the aforementioned elongated spread of near core pressure isobars. The strong wind speed values started to form and extend from the 976 hPa isobar line, which explains the wind speed differences over the Gulf of Riga stations and therefore the increase in surge height at Pärnu.

The SWAN hindcast simulation results for the 2013 storm also showed overestimation of  $H_s$  at the location of wave gauges (5.2 m vs. 7.3 m at NPB and 2.8 m vs. 4.5 m at GOF for observation and hindcast, respectively; Fig. 17). The problems of comparison were quite similar to those already described in case of 2005 storm wave modelling. It should



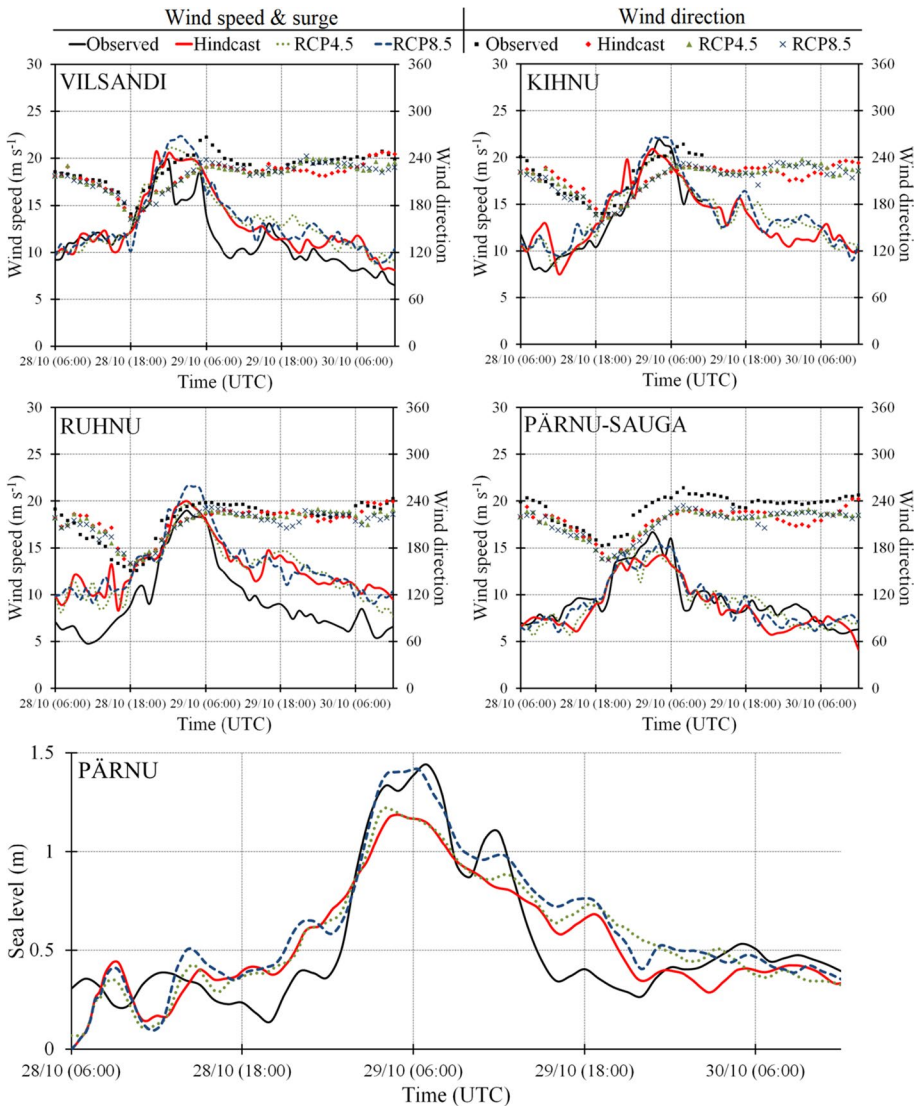


**Fig. 15** Modelling results for the 2013 storm St. Jude (see also Fig. 11)

also be noted that in terms of modelling it is challenging to achieve high accuracy when considering the complex configuration of the study area.

In terms of future simulations, the changes were not as apparent as they were for the stronger 2005 storm Gudrun. However, a small increase in  $H_s$  maximum (7.8 m vs. 7.4 m; Fig. 18) can be still seen. Also a slight south-ward extension of high wave fields occurred within the Baltic Proper. The expanded effect of the high wave zone could be more pronounced in the most extreme storm events (i.e. 2005 Gudrun; Fig. 14) and less so for weaker but still strong storms (i.e. 2013 St. Jude; Fig. 18).

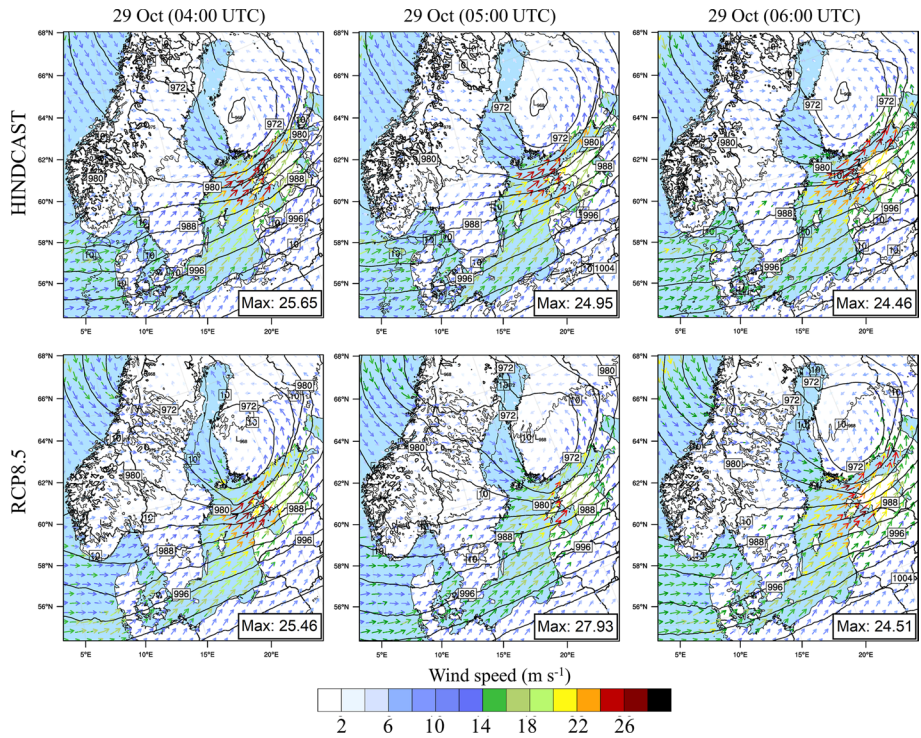


**Fig. 16** Wind and MSLP fields over WRF d02 for hindcast and RCP8.5 simulations (2013 case; see also Fig. 12)

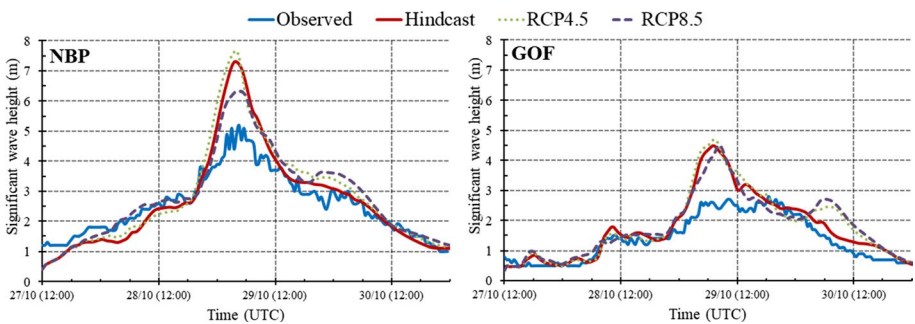


**Fig. 17** SWAN simulation and observed significant wave height comparisons at the two wave gauge stations (see also Fig. 4)

### 4.4 Wind according to the 2010 storm Xynthia (no surge)

The 2010 storm had the potential to elevate sea levels to a certain degree; however, in the late February the Estonian archipelago was locked by sea ice. Furthermore, the storm was considerably weakened once it arrived in the Baltic Sea region, and therefore, the main interest for that storm was to investigate wind and precipitation changes. The hindcast

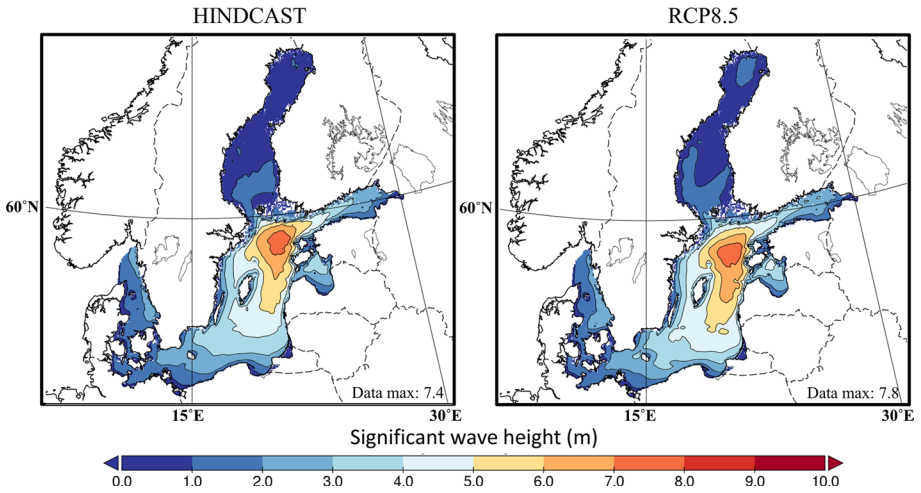


**Fig. 18** Spatial distribution of SWAN simulation results for the hindcast and RCP8.5 case at Oct-29 04:00 UTC, during the occurrence of highest simulated significant wave heights

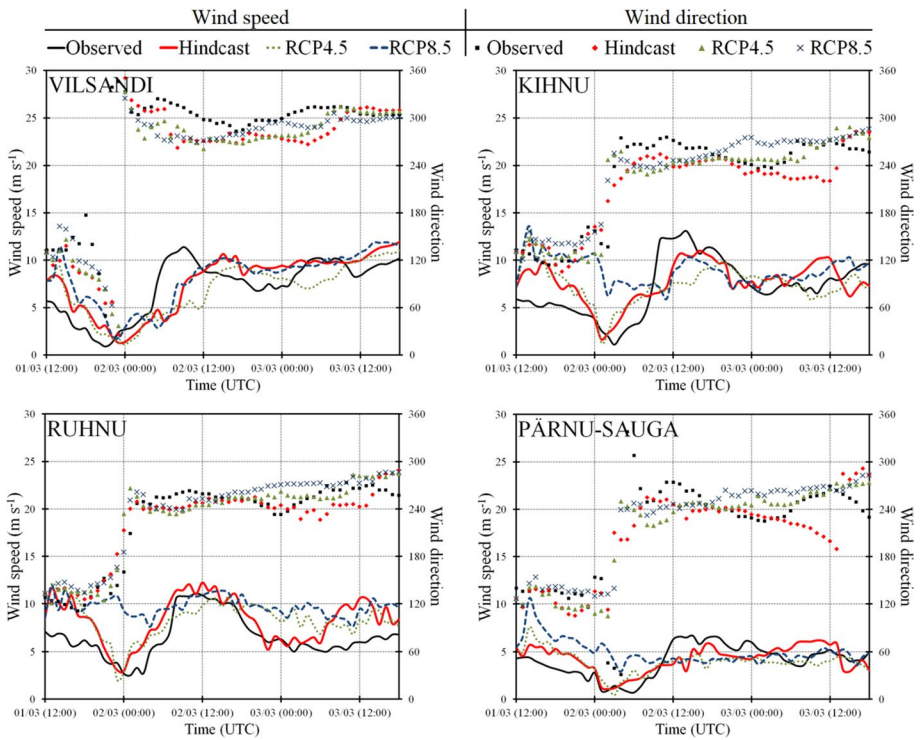


**Fig. 19** Simulation results for the 2010 storm Xynthia

simulations at four weather stations showed reasonably good results (Fig. 19), considering that modelling in general tends to have some difficulty in capturing weak synoptic patterns and winds. Overestimation of weaker winds occurred at the beginning and at the end phases of the simulations, whereas peak winds were well captured. Moreover, local natural or man-made obstructions (e.g. lighthouse at Vilsandi) in the vicinity of the stations can affect the actual measurements, while numerical models are not supposed to capture those local factors. Similarly, most stations, at times, showed model wind direction deviations as high as 50° (Fig. 19; Kihnu and Pärnu-Sauga). Also, the friction due to local dampening objects may easily turn the observed (weak) wind directions.

The future simulations aimed to study whether ETCs, travelling from far SW section of Europe, would reach north Europe as stronger systems. According to current study results, the “future storm Xynthia” would not. The 2010 storm started out as a subtropical cyclone (Liberato et al. 2013) and transitioned into ETC soon after its formation. The results on atmospheric pressure and winds, however, were not much different from the 2005 and 2013 cases. The RCP4.5 scenarios showed little to no change, whereas simulations with the RCP8.5 initially showed increased wind speeds over the Ruhnu and Kihnu stations (Fig. 19), although after 18 h the effect decreased.

#### 4.5 Precipitation changes (all events)

Firstly, the 2008 storm featured by low minimum sea level pressure and high precipitation. The comparison of minimum observed and modelled atmospheric pressures above Estonia yielded good results. The minimum pressure (both measured and modelled) was approximately 951 hPa, and the corresponding differences were rather small (average 1.1 hPa) at the mainland stations. Up to 8 hPa deviations occurred at the western Estonian coastline and island stations. Over the period of 96 h (22–25 November 2008), the accumulated precipitation amount in different Estonian weather stations varied between 15 and 37 mm in water equivalence. The average above the mainland was 29 mm, and the average considering also the islands (altogether 23 stations) was 25 mm. Despite “patchy”

**Table 5** Future scenario (year ~2090) area-total precipitation averages and corresponding changes (values in brackets) relative to hindcast for the 2008 storm case

	Av. (mm)	%	Av. (mm)	%
	2005		2008	
d01 RCP4.5	14.65 (+0.79)	5.4	17.52 (+0.61)	3.5
d02 RCP4.5	26.65 (+1.45)	5.2	16.72 (+0.71)	4.3
d03 RCP4.5	15.4 (+0.54)	3.5	24.46 (−1.49)	−6.1
d01 RCP8.5	15.01 (+1.14)	7.6	22.88 (+5.96)	27.3
d02 RCP8.5	28.61 (+3.40)	11.9	19.09 (+3.08)	16.1
d03 RCP8.5	18.6 (+3.74)	20.1	25.08 (−0.87)	−3.5
	2010		2013	
d01 RCP4.5	19.52 (+0.72)	3.7	15.97 (+0.59)	3.7
d02 RCP4.5	18.25 (+0.77)	4.2	23.14 (+2.33)	10.1
d03 RCP4.5	17.88 (+0.35)	1.9	21.8 (+0.85)	3.9
d01 RCP8.5	20.31 (+1.50)	7.4	16.61 (+1.23)	7.4
d02 RCP8.5	19.86 (+2.38)	11.9	25.38 (+4.57)	18
d03 RCP8.5	20.21 (+2.67)	13.2	27.11 (+6.16)	22.7

nature in precipitation distribution, the WRF modelled, area-weighted average precipitation amounted for 25.1 mm over the similar area.

Considering all four storm cases, the future changes remained rather modest and unclear under the RCP4.5 scenario (Table 5). The RCP8.5 simulations exhibited more clear tendencies. The three Atlantic storms (I–III, Fig. 1) showed steady precipitation increase from d01 to d03, while for the southerly 2008 storm it was the other way around (d01 highest and d03 the least). Furthermore, the homogeneous domains used for the Atlantic storms showed that over parent domain the increase for these storms was roughly the same, with average increase of 7.5%, regardless of the precipitation potential for these storms. The second domain that encompasses Baltic Sea and its surrounding countries showed 12–18% increase in total precipitation values (Table 5; Fig. 20). For the Estonian west coast (d03), the increase was between 13 and 23%. Among the three storms approaching from the Atlantic, the highest increase for the study area was for the 2013 October storm. However, the 2010 storm was already considerably weakened when it approached the domain 2, whereas the 2005 storm was at its strongest and the almost 12% precipitation increase for an already strong cyclonic system could potentially cause far more serious outcomes. For the 2005 and 2013 storms (both approaching from W-SW), an orographic enhancement of precipitation occurred over the Scandinavian mountains (Fig. 20).

Thus, according to the projections, westerly storms will all bring more precipitation to the study area, while the southerly storm case showed somewhat mixed results. In 2008 storm case, more precipitation occurred within the larger domains, and less in the smallest domain, covering a slightly larger area than Estonian territory (Table 5). As the atmospheric temperature will increase by 2°–3° by that time (~2090; Figs. 8, 9), the majority of precipitation would be in liquid form, not in snow. Future increase in cyclone-related rainfall amounts found in pseudo-climate change simulations was also predicted e.g. by Patricola and Wehner (2018).

#### 4.6 A new outlook versus study by Mäll et al. (2017)

According to the main results of this study, the authors must somewhat reconsider the previous study results, which suggested that the future ETCs might not get stronger in the region of the Baltic Sea. The current study showed that although no notable changes took place in minimum atmospheric pressure values within the ETCs of the future, the low pressure area was somewhat larger and the strong wind zone was extending further south with slightly higher peak wind speeds, especially in the case of RCP8.5. This, in turn, yielded a slight (3–18 cm) surge height increase at Pärnu under RCP4.5 scenario, and a more pronounced (22–59 cm) surge increase under RCP8.5 scenario. The different results this time were obtained due to a more advanced modelling system, and due to use of multi-model ensemble of 14 GCMs as opposed to a single GCM model in the previous study. It is difficult to estimate the uncertainty degree in one model simulation. In multi-model approach, it is virtually impossible to decide which one of the models is the “right one”, either. However, some guidance can be gained considering the scatter within the applied GCMs (Fig. 10 and Table 3).

Surge height increase occurred already in RCP4.5, but it was small, and against model scatter (Table 3), insignificant. The surge increase under RCP8.5, however, was more substantial (Table 4). A small increase in wave heights was also projected. Although the RCP8.5 future scenario is usually considered rather steep (i.e. pessimistic), it still shows that ETC-related storm surges can increase under warmer climates just like in the case of



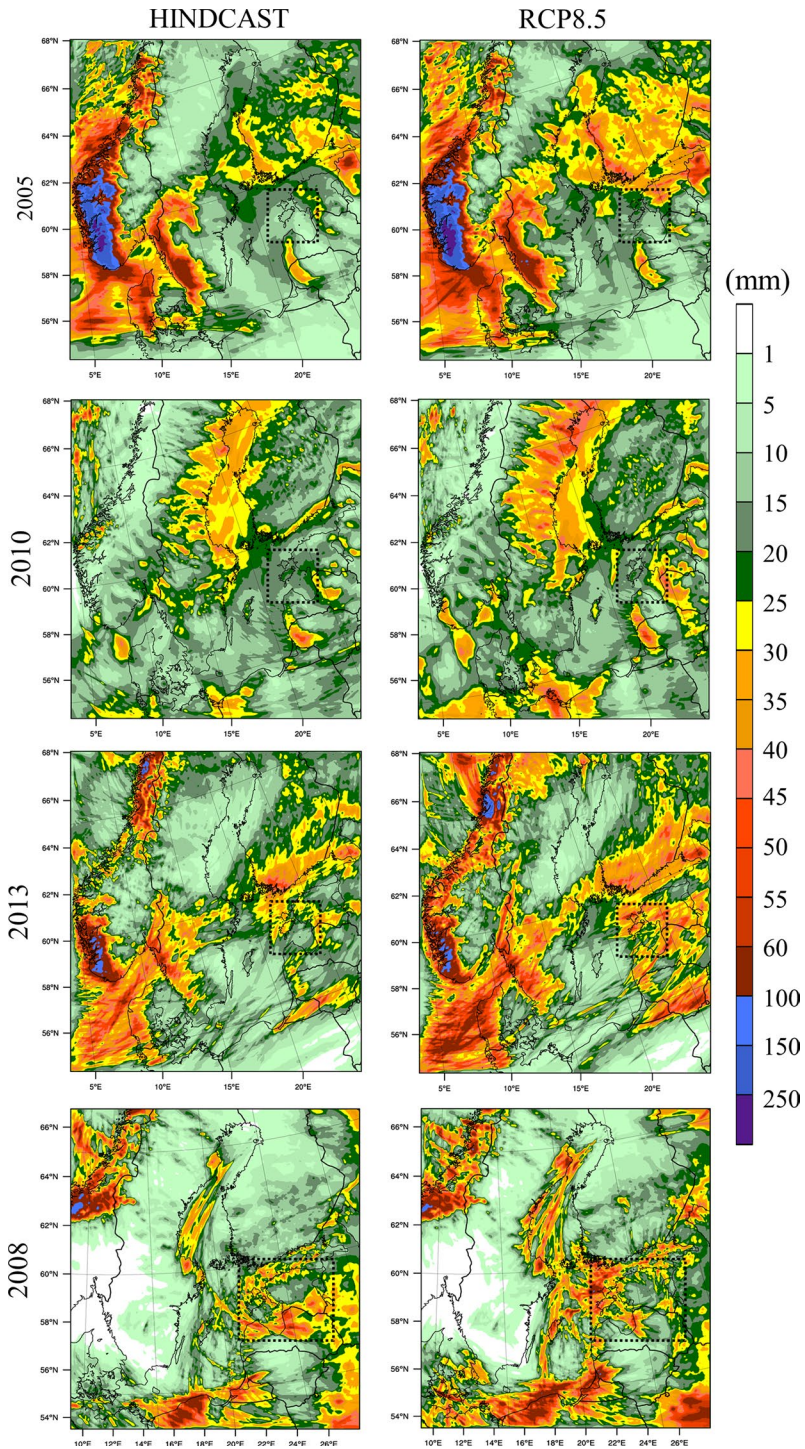


**Fig. 20** Total precipitations spatial distribution comparisons of hindcast and RCP8.5 scenarios over WRF domain 2. The dashed bounding boxes show the location of WRF d03



tropical cyclones (e.g. Nakamura et al. 2016). Perhaps, even if the pressure gradients at the polar front will not increase in the future due to warm-up of the polar regions (as suggested e.g. by Harvey et al. 2014), the increased global temperature (IPCC 2014) may still give growth to ETCs. However, this study merely presented the simulation results, but is not able to point on exact underlying processes in atmosphere physics.

Precipitation changes, not calculated in the previous study, showed that westerly approaching storms will bring more precipitation to the Baltic Sea area in the (warmer) future (Table 5). In case of southerly cyclones, the results were more mixed, but some increases could be expected there, too. Considering the results of four different storm cases, it is plausible that the extreme ETCs could become more severe and dangerous, at least under the most extreme emission scenario RCP8.5. Storms passing the Scandinavian mountains leave more precipitation there through orographic enhancement. Storm surge and increased fluvial risks as a result of increased precipitation can magnify each other impact on low-lying coastal communities locating in the river mouth areas (e.g. in the Pärnu city; Tönisson et al. 2019).

The current study also highlighted the importance of the initial and boundary conditions quality used for such modelling approach. The study by Mäll et al. (2017) employed quite similar calculation conditions as Nakamura et al. (2016) used for the 2013 tropical cyclone Haiyan. There, the results showed notable increase in storm intensity, whereas for a strong ETC (2005 Gudrun), no changes were captured. This indicated that one course calculation set-up might be sufficient for capturing changes in tropical cyclones, but more resolved atmospheric calculation conditions are necessary to capture changes in ETCs. The most notable improvements in this study, compared to the previous one, which led to the different results, were: (1) higher resolution meteorological data (CFSR vs. FNL), (2) larger simulation domains, (3) more meteorological grid levels (38 vs 27), (4) more vertical layers (61 vs 30 layers), (5) increased pressure top (1 hPa vs 50 hPa), (6) increased horizontal resolutions (20 vs 22.5 km; parent grid/time-step ratio: (5), (7) number of CMIP5 GCMs (14 vs 1), (8) surge model (FVCOM-SWAVE vs FVCOM) and (9) inclusion of wave model SWAN for the entire Baltic Sea.

## 5 Conclusions

In order to estimate the possible parameters of future ETCs, a pseudo-climate modelling study of four historic storms was performed using multi-model approach and considering the twenty-first centuries RCP4.5 and RCP8.5 emissions scenarios. The changes in cyclone parameters under future (2081–2100 avg. minus 2006–2015 avg. interpolated to reanalysis data) conditions in relation to hindcasted (present; NCEP CFSR/v2) conditions were calculated using WRF model, whereas FVCOM-SWAVE and SWAN models were used for estimating future storm surges at Pärnu (Estonia) and wave fields within the Baltic Sea, respectively. All the studied storms occurred during different thermal conditions (months) and responses somewhat varied.

As there was a high variability among the individual GCM models (14 CMIP5 models), it was necessary to use multi-model ensemble approach and not to rely on a single model. Compared to RCP4.5, the RCP8.5 scenario yielded much more pronounced future changes in virtually every aspect. The increase in domain-average weighed RCP4.5 and RCP8.5 was roughly 2°K vs. 4°K correspondingly (with mixed results in terms of humidity).

Regarding precipitation changes during the storms, the RCP4.5 scenario showed small tendencies ranging between  $-6$  and  $+10\%$ . Under RCP8.5, the total precipitation during the Atlantic storms increased  $\sim 7\%$  over the widest domain,  $12\text{--}18\%$  over the Baltic Sea domain and  $13\text{--}23\%$  over Estonia. Although during the 2008 (southerly) storm the results were somewhat mixed, some overall increase in precipitation could be still expected there, whereas the westerly approaching ETCs will very likely bring much more precipitation to the Baltic Sea area in the (warmer) future.

No notable changes took place in minimum atmospheric pressure values within the ETCs of the future, but the low pressure area was somewhat larger and the strong wind zone extended farther south. There were little to no changes in peak wind speeds under the RCP4.5 scenario; however, notable changes occurred under RCP8.5 scenario. This, in turn, yielded a small surge height increase at Pärnu under RCP4.5, but significant, up to  $22\text{--}59$  cm surge increase under RCP8.5 simulations. Besides wind speed increment, this increase could occur due to peak wind zone shift to better satisfy the optimum exposure conditions of Pärnu Bay. Under RCP8.5 scenario, an (insignificant) increase in maximum wave heights during extreme storms occurred. Along with the strong wind area spread from the cyclone core, also the higher wave areas extended further south and over larger sea areas. This, in turn, can also lead to increased hazards through wind damage and wave attacks along more extensive coastal stretches in the Baltic Proper. However, due to relatively large scatter of results and small number of analysed storms (four), these findings should serve as complementary information to possible climate change impacts, and not as definitive outcome.

Compared to results with previous work by Mäll et al. (2017), the different results regarding possible increase in surge height were obtained mainly due to use of multi-model ensemble of 14 GCMs as opposed to one model approach in the previous study, and due to improved initial and boundary conditions in the atmosphere model. Even if the steep RCP8.5 future scenario is usually considered as unrealistic, it still shows that the extreme ETCs could become more dangerous in case of substantial climate warming, and the related storm surges can increase, although probably not as certainly and as much, as in the case of tropical cyclones.

**Acknowledgements** The present work was performed as a part of activities of Research Institute of Sustainable Future Society, Waseda Research Institute for Science and Engineering, Waseda University. The study was financially supported by the Estonian Research Council Grant PUT1439, by Grant-in-Aid for Research Activity start-up (No. 17H06760) from Japan Society for the Promotion of Science and by Penta-Ocean Construction Co. Ltd. We also acknowledge the World Climate Research Programme's Working Group on Coupled Modelling, which is responsible for CMIP, and we thank the climate modelling groups (listed in Table 2) for producing and making available their model output. For CMIP, the US Department of Energy's Program for Climate Model Diagnosis and Intercomparison provides coordinating support and led development of software infrastructure in partnership with the Global Organization for Earth System Science Portals.

## References

- Averkiev AS, Klevannyi KA (2010) A case study of the impact of cyclonic trajectories on sea-level extremes in the Gulf of Finland. *Cont Shelf Res* 30:707–714
- Bertin X, Bruneau N, Breilh JF, Fortunato AB, Karpytchev M (2012) Importance of wave age and resonance in storm surges: the case Xynthia, Bay of Biscay. *Ocean Model* 42:16–30
- Björkqvist J-V, Lukas I, Alari V, van Vledder G, Hulst S, Pettersson H, Behrens A, Männik A (2018) Comparing a 41-year model hindcast with decades of wave measurements from the Baltic Sea. *Ocean Eng* 152:57–71

- Booij N, Ris RC, Holthuijsen LH (1999) A third-generation wave model for coastal regions: 1. Model description and validation. *J Geophys Res* 104(C4):7649–7666
- Chen C, Liu H, Beardsley RC (2003) An unstructured grid, finite-volume, three-dimensional, primitive equations ocean model: application to coastal ocean and estuaries. *J Atmos Ocean Technol* 20:159–186
- Christensen OB, Kjellström E, Zorita E (2015) Projected change—atmosphere. In: The BACC II Author Team (ed) Second assessment of climate change for the Baltic Sea Basin. Springer, Cham, pp 217–233
- Colle BA, Booth JF, Chang EKM (2015) A review of historical and future changes of extratropical cyclones and associated impacts along the US East Coast. *Curr Clim Change Rep* 1:125–143
- Emanuel K (2005) Increasing destructiveness of tropical cyclones over the past 30 years. *Nature* 436:686–688
- Feser F, Barcikowska M, Krueger O, Schenk F, Weisse R, Xia L (2015) Storminess over the North Atlantic and northwestern Europe—a review. *Q J R Meteorol Soc* 141:350–382
- Forbes C, Rhome J, Mattocks C, Taylor A (2014) Predicting the storm surge threat of hurricane sandy with the National Weather Service SLOSH model. *J Mar Sci Eng* 2:437–476
- Gregow H, Ruosteenoja K, Pimenoff N, Jylhä K (2012) Changes in the mean and extreme geostrophic wind speeds in Northern Europe until 2100 based on nine global climate models. *Int J Climatol* 32:1834–1846
- Grell GA, Freitas SR (2014) A scale and aerosol aware stochastic convective parameterization for weather and air quality modelling. *Atmos Chem Phys* 14:5233–5250
- Harvey BJ, Shaffrey LC, Woollings TJ (2014) Equator-to-pole temperature differences and the extratropical storm track responses of the CMIP5 climate models. *Clim Dyn* 43:1171–1182
- Hazeleger W, Van Den Hurk BJJM, Min E, Van Oldenborgh GJ, Petersen AC, Stainforth DA, Vasileiadou E, Smith LA (2015) Tales of future weather. *Nat Clim Change* 5(2):107–113
- Hoegh-Guldberg O, Bruno JF (2010) The impact of climate change on the World’s marine ecosystems. *Science* 328:1523–1528
- Honda C, Mitsuyasu K (1980) Laboratory study on wind effect to ocean surface. *J Coast Eng JSCE* 27:90–93 (in Japanese)
- Hong SY, Lim JOJ (2006) The WRF single-moment 6-class microphysics scheme (WSM6). *J Korean Meteorol Soc* 42:129–151
- Hong SY, Noh Y, Dudhia J (2006) A new vertical diffusion package with an explicit treatment of entrainment processes. *Mon Weather Rev* 134:2318–2341
- IPCC (2014) IPCC Fifth Assessment Report (AR5). <https://www.ipcc.ch/report/ar5/>
- Iacono M, Delamere J, Mlawer E, Shephard M, Clough S, Collins W (2008) Radiative forcing by long-lived greenhouse gases: calculations with the AER radiative transfer models. *J Geophys Res* 113:D13103
- Jaagus J, Suursaar Ü (2013) Long-term storminess and sea level variations on the Estonian coast of the Baltic Sea in relation to large-scale atmospheric circulation. *Est J Earth Sci* 62:73–92
- Jacob D, Elizalde A, Haensler A, Hagemann S, Kumar P, Podzun R, Rechied D, Remedio AR, Saeed F, Sieck K, Teichmann C, Wilhelm C (2012) Assessing the transferability of the regional climate model REMO to different coordinated regional climate downscaling experiment (CORDEX) regions. *Atmosphere* 3:181–199
- Jimenez PA, Dudhia J, Gonzalez-Rouco JF, Navarro J, Montavez JP, García-Bustamante E (2012) A revised scheme for the WRF surface layer formulation. *Mon Weather Rev* 140:898–918
- Kawase H, Yoshikane T, Hara M, Kimura F, Yasunari T, Ailikon B, Ueda H, Inoue T (2009) Intermodel variability of future changes in the Baiu rainband estimated by the pseudo global warming downscaling method. *J Geophys Res* 114:D24110
- Kimura F, Kitoh A (2007) Downscaling by pseudo global warming method. The Final Report of ICCAP, pp 43–46
- Knutson TR, Tuleya RE (2004) Impact of CO<sub>2</sub>-induced warming on simulated hurricane intensity and precipitation: sensitivity to the choice of climate model and convective parameterization. *J Clim* 17:3477–3495
- Liberato MLR, Pinto JG, Trigo RM, Ludwig P, Ordóñez P, Yuen D, Trigo IF (2013) Explosive development of winter storm Xynthia over the subtropical North Atlantic Ocean. *Nat Hazards Earth Syst Sci* 13:2239–2251
- Madsen O, Poon Y, Graber Y (1988) Spectral wave attenuation by bottom friction: theory. *Coast Eng Proc* 1:492–504
- Maraun D, Shepherd TG, Widmann M, Zappa G, Walton D, Gutiérrez JM, Hagemann S, Richter I, Soares PMM, Hall A, Mearns LO (2017) Towards process-informed bias correction of climate change simulations. *Nat Clim Change* 7:764–773
- Martin JE (2006) Mid-latitude atmospheric dynamics. Wiley, Hoboken

- Matulla C, Schöner W, Alexandersson H, von Storch H, Wang XL (2008) European storminess: late nineteenth century to present. *Clim Dyn* 31:125–130
- Mizuta R (2012) Intensification of extratropical cyclones associated with the polar jet change in the CMIP5 global warming projections. *Geophys Res Lett* 39:L19707
- Mäll M, Suursaar Ü, Nakamura R, Shibayama T (2017) Modelling a storm surge under future climate scenarios: case study of extratropical cyclone Gudrun (2005). *Nat Hazards* 89:1119–1144
- Mändla K, Jaagus J, Sepp M (2015) Climatology of cyclones with southern origin in northern Europe during 1948–2010. *Theor Appl Climatol* 120:75–86
- Nakamura R, Shibayama T, Esteban M, Iwamoto T (2016) Future typhoon and storm surges under different global warming scenarios: case study of typhoon Haiyan (2013). *Nat Hazards* 82:1645–1681
- Nevalainen K (2012) A case study of a snowstorm with multiple snowbands in southern Finland 23 November 2008 (Master's thesis). University of Helsinki, Faculty of Science, Department of Physics. Retrieved from <https://urn.fi/URN:NBN:fi-fe2017112251920>
- Patricola CM, Wehner MF (2018) Anthropogenic influences on major tropical cyclone events. *Nature* 563:339–346
- Pinto JG, Ulbrich U, Leckebusch GC, Spanghel T, Reyers M, Zacharias Kjellström E, Nikulin G, Hansson U, Strandberg G, Ullerstig A (2011) 21st century changes in the European climate: uncertainties derived from an ensemble of regional climate model simulations. *Tellus A* 63:24–40
- Post P, Köuts T (2014) Characteristics of cyclones causing extreme sea levels in the northern Baltic Sea. *Oceanologia* 56:241–258
- Qi J, Chen C, Beardsley RC, Perrie W, Cowles GW, Lai Z (2009) An unstructured-grid finite-volume surface wave model (FVCOM-SWAVE): implementation, validations and applications. *Ocean Model* 28:153–166
- Rauhala J, Juga I (2010) Wind and snow storm impacts on society. In: 15th International Road Weather Conference, Quebec City, Canada, 5–7 February 2010, 8 pp
- Roberts JF, Champion AJ, Dawkins LC, Hodges KI, Shaffrey LC, Stephenson DB, Stringer MA, Thornton HE, Youngman BD (2014) The XWS open access catalogue of extreme European windstorms from 1979 to 2012. *Nat Hazards Earth Syst* 14:2487–2501
- Sanders F, Gyakum JR (1980) Synoptic-Dynamic Climatology of the "Bomb". *Mon Weather Rev* 108:1589–1606
- Schär C, Christoph F, Lutthi D, Davies HC (1996) Surrogate climate-change scenarios for regional climate models. *Geophys Res Lett* 23:669–672
- Skamarock WC, Klemp JB, Dudhia J, Gill DO, Barker DM, Duda MG, Huang XY, Wang W, Powers JG (2008) A description of the advanced research WRF Version 3, NCAR Technical Note
- Stainforth DA, Alna T, Christensen C et al (2005) Uncertainty in the predictions of the climate response to rising levels of greenhouse gases. *Nature* 433:403–406
- Soomere T, Behrens A, Tuomi L, Nielsen JW (2008) Wave conditions in the Baltic Proper and in the Gulf of Finland during windstorm Gudrun. *Nat Hazards Earth Syst Sci* 8:37–46
- Sun Y, Chen C, Beardsley RC, Xu Q, Qi J, Lin H (2013) Impact of current-wave interaction on storm surge simulation: a case study for Hurricane Bob. *J Geophys Res Ocean* 118:2685–2701
- Suursaar Ü, Kall T (2018) Decomposition of relative sea level variations at tide gauges using results from four estonian precise levelings and uplift models. *IEEE J STARS* 11:1966–1974
- Suursaar Ü, Kullas T, Otsmann M (2002) A model study of sea level variations in the Gulf of Riga and the Väinameri Sea. *Cont Shelf Res* 22:2001–2019
- Suursaar Ü, Kullas T, Otsmann M, Saaremäe I, Kuik J, Merilain M (2006) Hurricane Gudrun and modelling its hydrodynamic consequences in the Estonian coastal waters. *Boreal Environ Res* 11:143–159
- Suursaar Ü, Jaagus J, Tõnisson H (2015) How to quantify long-term changes in coastal sea storminess? *Estuar Coast Shelf Sci* 156:31–41
- Suursaar Ü, Sepp M, Post P, Mäll M (2018) An inventory of historic storms and cyclone tracks that have caused met-ocean and coastal risks in the eastern Baltic Sea. *J Coast Res Spec Issue* 85:531–535. <https://doi.org/10.2112/S185-107.1>
- Tasnim KM, Shibayama T, Esteban M, Takagi H, Ohira K, Nakamura R (2015) Field observation and numerical simulation of past and future storm surges in the Bay of Bengal: case study of cyclone Nargis. *Nat Hazards* 75:1619–1647
- Tewari M, Chen F, Wang W, Dudhia J, LeMone MA, Mitchell K, Ek M, Gayno G, Wegiel J, Cuenca RH (2004) Implementation and verification of the unified NOAA land surface 677 model in the WRF model. In: 678 20th conference on weather analysis and forecasting/16th conference on numerical weather prediction (679), pp 1–15
- Trenberth K (2005) Uncertainty in hurricanes and global warming. *Science* 308:1753–1754

- Tõnisson H, Orviku K, Jaagus J, Suursaar Ü, Kont A, Rivis R (2008) Coastal damages on Saaremaa Island, Estonia, caused by the extreme storm and flooding on January 9, 2005. *J Coast Res* 24:602–614
- Tõnisson H, Kont A, Orviku K, Suursaar Ü, Rivis R, Palginõmm V (2019) Application of system approach framework for coastal zone management in Pärnu, SW Estonia. *J Coast Conserv* 23:931–942
- Ulbrich U, Leckebusch GC, Pinto JG (2009) Extra-tropical cyclones in the present and future climate: a review. *Theor Appl Climatol* 96:117–131
- Van Gelder PHAJM, Mai CV, Wang W, Shams G, Rajabalinejad M, Burgmeijer M (2008) Data management of extreme marine and coastal hydro-meteorological events. *J Hydraul Res* 46(Suppl. 2):191–210
- Viitak M, Maljutenko I, Alari V, Suursaar Ü, Rikka S, Lagemaa P (2016) The impact of surface currents and sea level on the wave field evolution during St. Jude storm in the eastern Baltic Sea. *Oceanologia* 58:176–186
- Vousdoukas MI, Voukouvalas E, Annunziato A, Giardino A, Feyen L (2016) Projections of extreme storm surge levels along Europe. *Clime Dyn*. <https://doi.org/10.1007/s00382-016-3019-5>
- Weisse R, von Storch H, Callies U, Chrastansky A, Feser F, Grabemann I, Günther H, Pluess A, Stoye T, Tellkamp J, Winterfeldt J, Woth K (2009) Regional meteorological–marine reanalyses and climate change projections. *Bull Am Meteorol Soc* 90:849–860
- Wolski T, Wiśniewski B, Giza A, Kowalewska-Kalkowska H, Boman H, Grabbi-Kaiv S, Hammarklint T, Holfort J, Lydeikaite Ž (2014) Extreme sea levels at selected stations on the Baltic Sea coast. *Oceanologia* 56:259–290
- Wu J (1982) Wind-stress coefficients over sea surface from Breeze to Hurricane. *J Geophys Res* 87:9704–9706
- Wu L, Chen C, Guo P, Shi M, Qi J, Ge J (2010) A FVCOM-based unstructured grid wave, current, sediment transport model, I. Model description and validation. *J Ocean Univ China* 10:1–8
- Woollings T, Hoskins B, Blackburn M, Hassell D, Hodges K (2010) Storm track sensitivity to sea surface temperatures resolution in a regional atmosphere model. *Clim Dyn* 35:343–353
- Zappa G, Shaffrey LC, Hodges KI (2013a) The ability of CMIP5 models to simulate North Atlantic extratropical cyclones. *J Clim* 26:5379–5396
- Zappa G, Shaffrey LC, Hodges KI, Sansom PG, Stephenson DB (2013b) A multi-model assessment of future projections of north atlantic and european extratropical cyclones in the CMIP5 climate models. *J Clim* 26:5846–5862

**Publisher's Note** Springer Nature remains neutral with regard to jurisdictional claims in published maps and institutional affiliations.